

Poisson-Bracket Approach to the Construction of Energy- and Potential-Enstrophy-Conserving Algorithms for the Shallow-Water Equations

RICK SALMON

Scripps Institution of Oceanography, University of California, San Diego, La Jolla, California

(Manuscript received 11 September 2003, in final form 27 February 2004)

ABSTRACT

Arakawa and Lamb discovered a finite-difference approximation to the shallow-water equations that exactly conserves finite-difference approximations to the energy and potential enstrophy of the fluid. The Arakawa–Lamb (AL) algorithm is a stunning and important achievement—stunning, because in the shallow-water case, neither energy nor potential enstrophy is a simple quadratic, and important because the simultaneous conservation of energy and potential enstrophy is known to prevent the spurious cascade of energy to high wavenumbers. However, the method followed by AL is somewhat ad hoc, and it is difficult to see how it might be generalized to other systems.

In this paper, the AL algorithm is rederived and greatly generalized in a way that should permit still further generalizations. Beginning with the Hamiltonian formulation of shallow-water dynamics, its two essential ingredients—the Hamiltonian functional and the Poisson-bracket operator—are replaced by finite-difference approximations that maintain the desired conservation laws. Energy conservation is maintained if the discrete Poisson bracket retains the antisymmetry property of the exact bracket, a trivial constraint. Potential enstrophy is conserved if a set of otherwise arbitrary coefficients is chosen in such a way that a very large quadratic form contains only diagonal terms. Using a symbolic manipulation program to satisfy the potential-enstrophy constraint, it is found that the energy- and potential-enstrophy-conserving schemes corresponding to a stencil of 25 grid points contain 22 free parameters. The AL scheme corresponds to the vanishing of all free parameters. No parameter setting can increase the overall accuracy of the schemes beyond second order, but 19 of the free parameters may be independently adjusted to yield a scheme with fourth-order accuracy in the vorticity equation.

1. Introduction

In a remarkable paper, Arakawa and Lamb (1981, hereafter AL) discovered a finite-difference scheme for the shallow-water equations that—apart from errors associated with the finite time step—exactly conserves finite-difference analogs of the energy and potential enstrophy of the flow. The practical importance of retaining energy- and enstrophy-conservation laws in numerical models had been appreciated since the earlier work of Arakawa (1966) on two-dimensional, nondivergent flow; but whereas the derivation of Arakawa’s Jacobian for nondivergent flow may be transparently understood in a variety of ways (see, e.g., Salmon and Talley 1989), the AL algorithm for shallow-water dynamics remains a stunning and somewhat mysterious achievement. In the case of two-dimensional, nondivergent flow, both the energy and enstrophy are relatively simple quadratic functionals of the streamfunction. However, in the shallow-water case, the energy (2.3) is a cubic functional of the velocity and depth, while the

potential enstrophy (2.10) involves a quotient. The existence of a numerical scheme that conserves analogs of both quantities is therefore somewhat surprising.

In deriving their scheme, AL followed the relatively straightforward strategy of posing finite-difference equations containing many arbitrary weights, and then choosing the weights in such a way that the conservation laws were maintained. However, success evidently required the inclusion of some highly unusual terms, namely, *unphysical* Coriolis terms of the form fu in the equation for $\partial u/\partial t$, and fv in the equation for $\partial v/\partial t$. These terms turned out to be consistently small, but their presence is apparently indispensable. In introducing the unphysical terms into their initial ansatz, AL remark only that the unphysical Coriolis terms “... give additional generality to the scheme ...” and “... should vanish when the grid size approaches zero as required for consistency”—a rather coy motivation for what appears to be a crucial step!

In this paper we rederive and greatly generalize the AL algorithm using the machinery of Hamiltonian mechanics. Our strategy is to replace the Poisson bracket for the shallow-water equations by a finite-difference approximation that retains two key properties of the exact bracket: the antisymmetry property, which guar-

Corresponding author address: Rick Salmon, UCSD Dept. 0213, 9500 Gilman Drive, La Jolla, CA 92093-0213.
E-mail: rsalmon@ucsd.edu

antees that an *arbitrary* approximation to the energy is conserved, and the Casimir property that the Poisson bracket vanishes when either of its two functional arguments is potential enstrophy. Following this strategy, we show that the problem of obtaining energy- and potential-enstrophy-conserving schemes reduces to the problem of choosing a set of coefficients in such a way that a very large quadratic form contains only diagonal terms. In the case of one space dimension, this problem is an easy one, and analysis yields a large, multiparameter family of conserving schemes. In the two-dimensional case, the problem is easy to pose but harder to analyze, and we use a symbolic manipulation program to diagonalize the quadratic form.

The resulting large, multiparameter set of two-dimensional, conserving, shallow-water algorithms contains the AL scheme, as well as the scheme discovered by Takano and Wurtele (1982, hereafter TW). These two schemes appear to be the only energy- and potential-enstrophy-conserving schemes known for shallow-water dynamics until the work of Abramopoulos (1988), who derived a large number of conserving schemes using a method based on "operator theory." Abramopoulos's method is similar to ours in that it makes extensive use of computer algebra. However, our method, which quickly reduces to the solution of a linear system, appears much easier to code, and may yet yield to analytical solution. Moreover, unlike Abramopoulos, we can present our results completely in a single table. The strategy of seeking conserving numerical schemes by discretizing the Poisson bracket was previously suggested by Szunyogh (1993), but he did not proceed further than verifying that three previously known schemes (none of which apply to general shallow-water flow) fit the Poisson-bracket form. The search for particular energy- and potential-enstrophy-conserving schemes continues right up to the present (see Ringler and Randall 2002).

Whenever conservation laws are at issue, Hamiltonian methods are the clear methods of choice; according to Noether's classic theorem, the conservation laws of a Hamiltonian system correspond directly to the symmetry properties of its Hamiltonian. Motivated by this correspondence, Salmon (1988, 1998) offered a general method for deriving approximate fluid-dynamical equations that retain the conservation laws of a more exact "parent" dynamics. The key idea was to make all the approximations directly on the Lagrangian of the parent system, taking care not to disturb symmetry properties that correspond to desired conservation laws. While this method was proposed for continuous systems described by differential equations, it is tempting to think that it could somehow be generalized to approximations that consist of replacing the continuous system by a discrete set of gridded variables. Unfortunately, however, the conservation of potential vorticity on fluid particles (from which potential-enstrophy conservation descends) corresponds to a symmetry property that amounts to a

continuous relabeling of the fluid particles. This seems to be the primary reason why Hamiltonian methods have not been especially helpful in constructing numerical schemes that conserve quantities (like potential enstrophy) related to potential vorticity. The present work was motivated by a strong desire to change this situation.

The paper is organized as follows. Section 2 provides the necessary background in Hamiltonian fluid dynamics, emphasizing the generic importance of the shallow-water Poisson bracket. Section 3 illustrates our basic idea by applying it to the one-dimensional shallow-water equations. Unfortunately, the simplified approach of section 3 does not apply successfully to the two-dimensional case, and in section 4 we derive general equations that determine the two-dimensional bracket. Specializing once again to the case of one dimension, we solve these general equations to obtain the general, conserving, one-dimensional bracket in section 5. The general one-dimensional bracket illuminates the structure of the two-dimensional bracket, which is obtained, using computer algebra, in section 6. There we find that the two-dimensional, energy- and potential-enstrophy-conserving bracket corresponding to an arbitrarily chosen stencil of moderate size contains 22 free parameters. No parameter setting can completely eliminate unphysical Coriolis terms of the kind originally introduced by AL. However, 19 of the free parameters may be independently adjusted to yield fourth-order accuracy in the vorticity equation. Section 6 compares the potential vorticity field computed with six distinct conserving schemes, finding that schemes with the same accuracy yield very similar results despite quite significant differences in the form of the bracket. Section 7 concludes with a philosophical discussion.

2. Background

The shallow-water equations may be written in the form

$$u_t - qhv = -\Phi_x, \quad (2.1a)$$

$$v_t + qhu = -\Phi_y, \quad (2.1b)$$

$$h_t + (hu)_x + (hv)_y = 0, \quad (2.1c)$$

where $(u, v) = \mathbf{u}(x, y, t)$ is the velocity in the (x, y) direction at time t , h is the fluid depth, $\Phi = (1/2)u^2 + (1/2)v^2 + gh$, g is the gravity constant, and $q = (v_x - u_y)h^{-1}$ is the potential vorticity. All of our results hold also for the case of rotating flow, in which the numerator of q includes a Coriolis-parameter term. In a slight departure from the standard terminology, we shall call the q terms in (2.1a) and (2.1b) *Coriolis terms*. For boundary conditions, we take the flow to be periodic in x and y .

The dynamics (2.1) is equivalent to

$$\frac{dF}{dt} = \{F, H\}, \quad (2.2)$$

where $F[u, v, h]$ is an arbitrary functional of the dependent variables $u(x, y, t)$, $v(x, y, t)$, and $h(x, y, t)$;

$$H = \iint d\mathbf{x} \left(\frac{1}{2}hu^2 + \frac{1}{2}hv^2 + \frac{1}{2}gh^2 \right) \quad (2.3)$$

is the Hamiltonian of the shallow-water system; and

$$\{A, B\} = \iint d\mathbf{x} \left[q \frac{\delta(A, B)}{\delta(u, v)} - \frac{\delta A}{\delta \mathbf{u}} \cdot \nabla \frac{\delta B}{\delta h} + \frac{\delta B}{\delta \mathbf{u}} \cdot \nabla \frac{\delta A}{\delta h} \right] \quad (2.4)$$

is the Poisson bracket, defined for any two functionals A and B . Here, $\nabla = (\partial_x, \partial_y)$, $\delta A/\delta u$ is the functional derivative of A with respect to u , and

$$\frac{\delta(A, B)}{\delta(u, v)} = \frac{\delta A}{\delta u} \frac{\delta B}{\delta v} - \frac{\delta B}{\delta u} \frac{\delta A}{\delta v} \quad (2.5)$$

is the functional Jacobian. Thus, for example,

$$\begin{aligned} U &\equiv \frac{\delta H}{\delta u} = hu, & V &\equiv \frac{\delta H}{\delta v} = hv, \\ \Phi &\equiv \frac{\delta H}{\delta h} = \frac{1}{2}u^2 + \frac{1}{2}v^2 + gh, \end{aligned} \quad (2.6)$$

and using (2.2) we find that

$$\begin{aligned} \frac{\partial}{\partial t} u(\mathbf{x}_0, t) &= \{u(\mathbf{x}_0, t), H\} \\ &= \iint d\mathbf{x} \left[q \delta(\mathbf{x} - \mathbf{x}_0) \frac{\delta H}{\delta v} - \delta(\mathbf{x} - \mathbf{x}_0) \frac{\partial}{\partial x} \frac{\delta H}{\delta h} \right] \\ &= qhv(\mathbf{x}_0, t) - \left. \frac{\partial \Phi}{\partial x} \right|_{\mathbf{x}_0}, \end{aligned} \quad (2.7)$$

in agreement with (2.1a).

Energy is conserved,

$$\frac{dH}{dt} = \{H, H\} = 0, \quad (2.8)$$

because the Poisson bracket (2.4) is antisymmetric in its two arguments. However, the dynamics (2.2) also conserves Casimirs of the form

$$C = \iint d\mathbf{x} hG(q), \quad (2.9)$$

where G is an arbitrary function of the potential vorticity q . Important special cases of (2.9) include the mass $\iint d\mathbf{x} h$, the circulation $\iint d\mathbf{x} hq$, and the potential enstrophy

$$Z = \frac{1}{2} \iint d\mathbf{x} hq^2 = \frac{1}{2} \iint d\mathbf{x} (v_x - u_y)^2 h^{-1}. \quad (2.10)$$

The conservation of (2.9) follows from the property of the Poisson bracket (2.4) that

$$\{A, C\} = 0 \quad (2.11)$$

for any functional A . The Poisson bracket also obeys the Jacobi identity

$$\{A, \{B, D\}\} + \{B, \{D, A\}\} + \{D, \{A, B\}\} = 0 \quad (2.12)$$

for any three functionals A, B , and D . For further background on Hamiltonian fluid dynamics and Poisson brackets, refer to Shepherd (1990), Morrison (1998), or Salmon (1998).

We construct discrete analogs of the shallow-water equations by replacing the Hamiltonian (2.3) and Poisson bracket (2.4) by discrete approximations. The conservation of energy and potential enstrophy depend solely on the form of the discrete bracket. Energy is conserved if the discrete bracket retains the antisymmetry property of (2.4), a trivial constraint. Potential enstrophy is conserved if the discrete bracket retains the property $\{A, Z\} = 0$ for arbitrary A ; this second constraint proves highly nontrivial.

Our results apply to systems much more general than the one-layer shallow-water equations (2.1), because the shallow-water bracket (2.4) is the *standard noncanonical bracket* for all two-dimensional fluids. By this we mean the following. If, for any two-dimensional system, Hamilton's principle may be stated as

$$\begin{aligned} \delta \int d\tau \iint da db \left(u \frac{\partial x}{\partial \tau} + v \frac{\partial y}{\partial \tau} \right) \\ - H[x, y, u, v] = 0 \end{aligned} \quad (2.13)$$

for arbitrary independent variations in the locations δx , $\delta y(a, b, \tau)$ and momenta δu , $\delta v(a, b, \tau)$ of fluid particles labeled by (a, b) at time τ , and if the Hamiltonian is expressible as a functional $H[u, v, h]$ of the *reduced variables* u, v , and $h \equiv \partial(a, b)/\partial(x, y)$, then the dynamics may be expressed in the form (2.2)–(2.4) with (2.3) replaced by the general Hamiltonian in (2.13). The proof is a straightforward application of the chain rule for functional derivatives; for a similar proof, see Shepherd (1990, appendix). We recognize the x, y, u, v in (2.13) as canonical variables. Only the *form* of (2.13) is relevant to the proof; the *physical interpretation* of u and v is arbitrary. The one-layer shallow-water equations fit the form of (2.13) with (u, v) the velocity and h the fluid depth. Multilayer shallow water systems take a Hamiltonian form in which the Poisson bracket is the sum of brackets of the form (2.4) *for each layer*, and the Hamiltonian contains coupling terms between the layers. As another example, the Green–Naghdi equations (e.g., Salmon 1998, 313–318) fit the form of (2.13) with \mathbf{u} replaced by $\mathbf{u} + (1/3)h^{-1}\nabla(h^2 Dh/Dt)$.

For all of these examples, we obtain energy and potential-enstrophy-conserving numerical schemes by combining the brackets derived in this paper—with u and v regarded as the canonical momenta, and $h \equiv \partial(a, b)/\partial(x, y)$ —with the appropriate Hamiltonian writ-

ten in terms of these same variables. To shift from one two-dimensional dynamics to a completely different two-dimensional dynamics then only requires that the form of the Hamiltonian be changed.

Hamiltonian methods have seen relatively limited use in the construction of numerical algorithms. Most previous applications involve the construction of symplectic integrators—time-stepping algorithms that (loosely speaking) preserve volume conservation in phase space. Such applications begin with coupled ordinary differential equations that are assumed to be Hamiltonian. These ordinary differential equations *might* have been obtained—but never actually *are* obtained—by discretizing the space derivatives in field equations like (2.1). In fact it seems almost impossible to discretize Hamiltonian field equations in such a way that the Jacobi property (2.12) is maintained.¹ In this paper we abandon (2.12), thereby leaving the realm of true Hamiltonian systems, and we maintain potential-*enstrophy* conservation by stubborn insistence that the discrete bracket retain *some* of the Casimir properties of (2.4).

3. Preview in one dimension

To explain ideas in the simplest context, we first consider the case of one-dimensional flow, in which nothing varies in the *y* direction. In one dimension, the Poisson bracket (2.4) takes the form

$$\{A, B\} = \int dx \left[q \frac{\delta(A, B)}{\delta(u, v)} - \frac{\delta A}{\delta u} \frac{\partial}{\partial x} \frac{\delta B}{\delta h} + \frac{\delta B}{\delta u} \frac{\partial}{\partial x} \frac{\delta A}{\delta h} \right], \tag{3.1}$$

with $q = v_x h^{-1}$. We obtain finite-difference analogs of the one-dimensional shallow-water equations by replacing (3.1) and (2.3) by finite-difference approximations. Let Δ be the grid separation, and let u_i, v_i, h_i be the values at the *i*th grid point. Then the finite-difference approximation

$$\begin{aligned} \{A, B\} = \sum_i \frac{1}{2\Delta} & \left[\frac{(v_{i+1} - v_{i-1})}{h_i} \frac{\partial(A, B)}{\partial(u_i, v_i)} \right. \\ & - \frac{\partial A}{\partial u_i} \left(\frac{\partial B}{\partial h_{i+1}} - \frac{\partial B}{\partial h_{i-1}} \right) \\ & \left. + \frac{\partial B}{\partial u_i} \left(\frac{\partial A}{\partial h_{i+1}} - \frac{\partial A}{\partial h_{i-1}} \right) \right] \tag{3.2} \end{aligned}$$

to (3.1) yields the discrete dynamics

$$\frac{du_i}{dt} = \{u_i, H\} = q_i \frac{\partial H}{\partial v_i} - \frac{1}{2\Delta} \left(\frac{\partial H}{\partial h_{i+1}} - \frac{\partial H}{\partial h_{i-1}} \right), \tag{3.3a}$$

$$\frac{dv_i}{dt} = \{v_i, H\} = -q_i \frac{\partial H}{\partial u_i}, \tag{3.3b}$$

$$\frac{dh_i}{dt} = \{h_i, H\} = \frac{1}{2\Delta} \left(\frac{\partial H}{\partial u_{i-1}} - \frac{\partial H}{\partial u_{i+1}} \right), \tag{3.3c}$$

where

$$q_i = (2\Delta)^{-1} (v_{i+1} - v_{i-1}) h_i^{-1}, \tag{3.4}$$

and H is the yet-to-be-defined discrete Hamiltonian.² The simplest choice is undoubtedly $H = (1/2) \sum_i (h_i u_i^2 + h_i v_i^2 + g h_i^2)$. However, by the antisymmetry property of (3.2), the discrete dynamics (3.3) conserves H for any choice of H . The mass $\sum_i h_i$ and circulation $\sum_i (v_{i+1} - v_{i-1})/2\Delta$ are likewise conserved. However, the discrete potential enstrophy

$$Z = \frac{1}{2} \sum_i h_i q_i^2 = \frac{1}{2} \sum_i (v_{i+1} - v_{i-1})^2 (2\Delta)^{-2} h_i^{-1} \tag{3.5}$$

is *not* conserved by the dynamics (3.3).

To obtain a discrete dynamics that *does* conserve potential enstrophy, we generalize (3.2) to

$$\begin{aligned} \{A, B\} = \sum_i & \left[\tilde{q}_i \frac{\partial(A, B)}{\partial(u_i, v_i)} - \frac{\partial A}{\partial u_i} \frac{1}{2\Delta} \left(\frac{\partial B}{\partial h_{i+1}} - \frac{\partial B}{\partial h_{i-1}} \right) \right. \\ & \left. + \frac{\partial B}{\partial u_i} \frac{1}{2\Delta} \left(\frac{\partial A}{\partial h_{i+1}} - \frac{\partial A}{\partial h_{i-1}} \right) \right], \tag{3.6} \end{aligned}$$

where \tilde{q}_i is an as-yet-unspecified approximation to q_i . Energy, mass, and circulation are conserved for any choice of \tilde{q}_i and H . To obtain potential-*enstrophy* conservation, we attempt to choose \tilde{q}_i such that $\{A, Z\}$ vanishes for any A , where Z is given by (3.5). By the chain rule, it clearly suffices to require that $\{u_i, Z\} = \{v_i, Z\} = \{h_i, Z\} = 0$ for arbitrary i . The second and third of these equations are trivially satisfied, and the first is satisfied if

$$\tilde{q}_i \frac{\partial Z}{\partial v_i} - \frac{1}{2\Delta} \left(\frac{\partial Z}{\partial h_{i+1}} - \frac{\partial Z}{\partial h_{i-1}} \right) = 0. \tag{3.7}$$

From (3.5) we find that

$$\frac{\partial Z}{\partial v_i} = \frac{(q_{i-1} - q_{i+1})}{2\Delta}, \quad \frac{\partial Z}{\partial h_i} = -\frac{1}{2} q_i^2. \tag{3.8}$$

It follows from (3.7)–(3.8) that

¹ Exceptions to this statement include the familiar, canonical, point-vortex formulation of two-dimensional incompressible flow, and the discretizations proposed by Zeitlin (1991) for that same physics.

² In (3.3), as throughout this paper, we regard the time derivatives as exact. That is, we do not consider the loss of conservation properties that will result from replacing the time derivative by a finite difference. Experience shows that the errors introduced by time differencing are usually negligible in comparison to those introduced by space differencing.

$$\tilde{q}_i = \frac{1}{2}(q_{i-1} + q_{i+1}). \tag{3.9}$$

Suppose, instead of (3.5), we want the discrete dynamics to conserve the Casimir

$$Z = \sum_i h_i q_i^{-1} \tag{3.10}$$

corresponding to $G(q) = q^{-1}$ in (2.9). For (3.10) we obtain, instead of (3.8),

$$\frac{\partial Z}{\partial v_i} = \frac{1}{2\Delta}(q_{i+1}^{-2} - q_{i-1}^{-2}), \quad \frac{\partial Z}{\partial h_i} = 2q_i^{-1}, \tag{3.11}$$

for which (3.7) implies

$$\tilde{q}_i = 2q_{i-1}q_{i+1}(q_{i-1} + q_{i+1})^{-1} \tag{3.12}$$

instead of (3.9). More generally, the choice

$$\tilde{q}_i = (\lambda - 1)\lambda^{-1}(q_{i+1}^\lambda - q_{i-1}^\lambda)(q_{i+1}^{\lambda-1} - q_{i-1}^{\lambda-1})^{-1} \tag{3.13}$$

conserves the Casimir

$$Z = \lambda^{-1} \sum_i h_i q_i^\lambda. \tag{3.14}$$

All these conserved quantities are *global* invariants, expressed as sums over all the grid points. However, each global conservation law also corresponds to a *local* statement equating a time derivative to the difference of a flux. The existence of a local conservation law follows automatically from the global conservation law, and from the use of a relatively small stencil of nearby grid points in each summand of the discrete bracket.

Unfortunately, the problem of finding *two-dimensional* Casimir-conserving schemes proves much more difficult. Consider the obvious two-dimensional generalization of (3.6), and attempt to find \tilde{q}_{ij} , such that the potential enstrophy $Z = (1/2) \sum_i h_{ij} q_{ij}^2$ is a Casimir, where now

$$q_{ij} = (2\Delta)^{-1}(v_{i+1,j} - v_{i-1,j} - u_{i,j+1} + u_{i,j-1})h_{ij}^{-1}. \tag{3.15}$$

The equation $\{h_{ij}, Z\} = 0$ is still satisfied, but now $\{u_{ij}, Z\} = 0$ implies

$$\tilde{q}_{ij} = \frac{1}{2}(q_{i-1,j} + q_{i+1,j}), \tag{3.16}$$

whereas $\{v_{ij}, Z\} = 0$ implies

$$\tilde{q}_{ij} = \frac{1}{2}(q_{i,j-1} + q_{i,j+1}). \tag{3.17}$$

Of course, (3.16) and (3.17) cannot both be satisfied.

The difference between the naively chosen one-dimensional bracket (3.2) and the potential-enstrophy-conserving bracket (3.6) and (3.9) is that the latter replaces the term

$$\frac{\delta(A, B)}{q \delta(u, v)} \tag{3.18}$$

in (2.4) with an expression in which q and (u, v) are evaluated at different grid points. The key to success in two dimensions appears to be to generalize this approximation still further, replacing (3.18) by a sum of terms of the form

$$q_{ij} \frac{\partial(A, B)}{\partial(u_{kl}, v_{mn})} \tag{3.19}$$

in which *none* of q, u, v are necessarily evaluated at the same grid point.

4. The two-dimensional case

Pursuing this suggestion, we replace the exact Poisson bracket (2.4) by the approximation

$$\{A, B\} = \{A, B\}_Q + \{A, B\}_R, \tag{4.1}$$

where

$$\begin{aligned} \{A, B\}_Q = \sum_{\mathbf{x}} q_{\mathbf{x}} \sum_{\mathbf{n}, \mathbf{m}} & \left[\alpha_{\mathbf{nm}} \frac{\partial(A, B)}{\partial(u_{\mathbf{x}+\mathbf{n}}, v_{\mathbf{x}+\mathbf{m}})} \right. \\ & + \beta_{\mathbf{nm}} \frac{\partial(A, B)}{\partial(u_{\mathbf{x}+\mathbf{n}}, u_{\mathbf{x}+\mathbf{m}})} \\ & \left. + \gamma_{\mathbf{nm}} \frac{\partial(A, B)}{\partial(v_{\mathbf{x}+\mathbf{n}}, v_{\mathbf{x}+\mathbf{m}})} \right] \end{aligned} \tag{4.2}$$

is the discrete approximation to the q part of the bracket in (2.4), and

$$\begin{aligned} \{A, B\}_R = \frac{1}{2\Delta} \sum_{\mathbf{x}} & \left[\frac{\partial B}{\partial u_{\mathbf{x}}} \left(\frac{\partial A}{\partial h_{\mathbf{x}+\mathbf{i}}} - \frac{\partial A}{\partial h_{\mathbf{x}-\mathbf{i}}} \right) \right. \\ & \left. + \frac{\partial B}{\partial v_{\mathbf{x}}} \left(\frac{\partial A}{\partial h_{\mathbf{x}+\mathbf{j}}} - \frac{\partial A}{\partial h_{\mathbf{x}-\mathbf{j}}} \right) - (A \leftrightarrow B) \right] \end{aligned} \tag{4.3}$$

is the approximation to the remaining part of (2.4). Here,

$$q_{\mathbf{x}} = \zeta_{\mathbf{x}} \tilde{h}_{\mathbf{x}}^{-1} \tag{4.4}$$

is an approximation to the potential vorticity at grid point \mathbf{x} , and the sums over $\mathbf{x} = (i, j)$, where i and j are integers, represent sums over a square two-dimensional lattice. The quantity $\zeta_{\mathbf{x}}$ is an arbitrary finite-difference approximation to the relative vorticity; $\tilde{h}_{\mathbf{x}}$ is an approximation to $h_{\mathbf{x}}$. The sums over \mathbf{n} and \mathbf{m} represent sums over grid points near \mathbf{x} . That is, the coefficients $\alpha_{\mathbf{nm}}, \beta_{\mathbf{nm}}, \gamma_{\mathbf{nm}}$ vanish if $\mathbf{n} = (n_x, n_y)$ or $\mathbf{m} = (m_x, m_y)$ lies outside a relatively small prescribed set $\{(n_x, n_y)\}$ in which (for example), $|n_x|, |n_y| < M$, where M is a small integer; we call M the *stencil size* of the corresponding discrete algorithm. In (4.3), \mathbf{i} and \mathbf{j} are the unit vectors in the x and y direction, and the symbol $(A \leftrightarrow B)$ stands for the preceding expression with interchange of A and B .

The discrete bracket corresponding to the AL scheme takes the form of (4.1)–(4.4) with

$$\zeta_x \equiv \zeta_{i,j} = (2\Delta)^{-1}(v_{i+1,j} - v_{i-1,j} - u_{i,j+1} + u_{i,j-1}), \quad (4.5)$$

$$\tilde{h}_{i,j} = \frac{1}{4}(h_{i+1,j+1} + h_{i+1,j-1} + h_{i-1,j+1} + h_{i-1,j-1}), \quad (4.6)$$

and with 16 nonzero α_{nm} coefficients, 4 nonzero β_{nm} coefficients, and 4 nonzero γ_{nm} coefficients, as follows:

$$\begin{aligned} \alpha_{(0,1)(1,2)} &= \alpha_{(0,1)(-1,2)} = \alpha_{(0,-1)(1,-2)} = \alpha_{(0,-1)(-1,-2)} \\ &= \alpha_{(2,1)(1,0)} = \alpha_{(2,-1)(1,0)} = \alpha_{(-2,1)(-1,0)} \\ &= \alpha_{(-2,-1)(-1,0)} = 1/12, \end{aligned} \quad (4.7a)$$

$$\alpha_{(0,1)(1,0)} = \alpha_{(0,1)(-1,0)} = \alpha_{(0,-1)(1,0)} = \alpha_{(0,-1)(-1,0)} = 1/24, \quad (4.7b)$$

$$\begin{aligned} \alpha_{(2,1)(1,2)} &= \alpha_{(2,-1)(1,-2)} = \alpha_{(-2,-1)(-1,-2)} \\ &= \alpha_{(-2,1)(-1,2)} = 1/24, \end{aligned} \quad (4.7c)$$

$$\begin{aligned} \beta_{(0,1)(2,1)} &= \beta_{(2,-1)(0,-1)} = \beta_{(0,-1)(-2,-1)} = \beta_{(-2,1)(0,1)} \\ &= \gamma_{(1,2)(1,0)} = \gamma_{(1,0)(1,-2)} = \gamma_{(-1,-2)(-1,0)} \\ &= \gamma_{(-1,0)(-1,2)} = 1/24. \end{aligned} \quad (4.7d)$$

The β_{nm} and γ_{nm} terms in (4.2), which have no analogs in (2.4), are the source of the unphysical Coriolis terms in the AL scheme. But whereas the presence of these terms is a somewhat jarring aspect of the AL derivation, their occurrence in (4.2) seems almost unavoidable. This is because, unlike the scalars q and h , the variables u and v are the components of a vector. If we rotate, with respect to the square lattice, the coordinate system with respect to which u and v are defined, then u and v transform in such a way that β_{nm} and γ_{nm} terms would appear, if not already present. For example, a 45° rotation generates the transformations $u \rightarrow 2^{-1/2}(u + v)$ and $v \rightarrow 2^{-1/2}(v - u)$. Then, using the chain rule, we easily see that $\partial(A, B)/\partial(u_x, v_x)$ transforms into an expression that also contains $\partial(A, B)/\partial(u_x, u_x)$ and $\partial(A, B)/\partial(v_x, v_x)$, provided that $\mathbf{x} \neq \mathbf{x}'$. Thus, the a priori inclusion of β_{nm} and γ_{nm} terms seems to be a necessary consequence of the decision to approximate (3.18) by an expression involving staggered grid points.

More disturbing than the generality of (4.2) is the fact that the AL scheme corresponds to so many nonzero coefficients (4.7). Yet, as we shall see, (4.1)–(4.7) seems to be the simplest potential-entropy-conserving bracket. The complexity of (4.7) is greatly offset by the fact that only four of the coefficients in (4.7) are truly independent if we take the symmetry properties of α_{nm} , β_{nm} , and γ_{nm} into account. Before discussing these symmetry properties, we digress on the subject of grid systems.

By *grid system* we mean the set of discrete dependent variables that appear in a numerical scheme. The so-called A system uses all of the four variables u , v , h ,

and q at every gridpoint. The E system (Fig. 1e) uses (u, v) and (q, h) at alternate grid points. We view the E system as a decimated A system in which half of the A system variables have simply been discarded. Thus every A system contains two E systems, each defined by choosing one particular grid point to be a (u, v) point or a (q, h) point. A further decimation produces the C system, in which only one of u, v, h, q is defined at every gridpoint, in the pattern shown on Fig. 1c. Thus, every A system contains two E systems and four C systems. Each E system is equivalent to a B system, by a rotation and stretching of the lattice (Fig. 1b). These four seem to be the square-lattice systems in widest meteorological use. The designations A, B, C, E represent a well-established convention (see, e.g., Arakawa and Lamb 1977).

The AL scheme is a C system; this is the reason for the somewhat complicated form (4.6) of the denominator in (4.4). To maintain C system compatibility, the AL scheme uses the Hamiltonian

$$H = \sum_{\mathbf{x}} \left[\frac{1}{8} h_{\mathbf{x}} (u_{\mathbf{x}+1} + u_{\mathbf{x}-1})^2 + \frac{1}{8} h_{\mathbf{x}} (v_{\mathbf{x}+j} + v_{\mathbf{x}-j})^2 + \frac{1}{2} g h_{\mathbf{x}}^2 \right], \quad (4.8)$$

in which the sum runs only over h points, the grid points at which h is defined in Fig. 1c. Similarly, in the AL scheme, the sum over \mathbf{x} in (4.2) runs only over q points, and the sums in (4.3) are similarly restricted. Alternatively, we may regard the \mathbf{x} sums in (4.2), (4.3), and (4.8) as sums over *all* the grid points. Then the dynamics (4.1)–(4.8) corresponds to four *independent* AL schemes for four *interleaved* C systems. But if, instead of (4.8), we use the Hamiltonian

$$H = \sum_{\mathbf{x}} \left(\frac{1}{2} h_{\mathbf{x}} u_{\mathbf{x}}^2 + \frac{1}{2} h_{\mathbf{x}} v_{\mathbf{x}}^2 + \frac{1}{2} g h_{\mathbf{x}}^2 \right), \quad (4.9)$$

then the four C systems are coupled together. Although technically an A system, the resulting discrete equations are simpler than those proposed by AL, because the Hamiltonian (4.9) is simpler than (4.8).

This discussion illustrates an important advantage of the Hamiltonian approach, namely, the separation of dynamical structure into truly independent components. From the Hamiltonian viewpoint, the dynamics comprises two geometrical objects—the Poisson bracket (a bilinear operator) and the Hamiltonian (a scalar). In the discrete case, as in the continuous case, potential-entropy conservation is associated with the properties of the bracket. However, the simplest discrete bracket may be sought independently of the simplest discrete Hamiltonian, because the two objects *are* independent. We shall see that virtually all of the subtleties associated with the choice of bracket involve the part (4.2). In essence, the problem of finding discrete energy- and

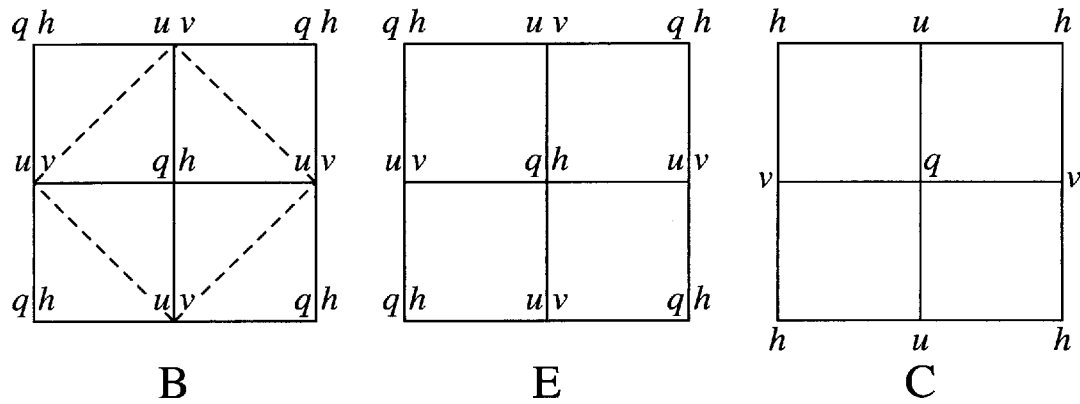


FIG. 1. The placement of the dependent variables on the various grid systems. The B grid may be viewed as a rotation of the E grid.

potential-entropy-conserving shallow-water schemes reduces to the problem of finding the coefficients α_{nm} , β_{nm} , and γ_{nm} in (4.2).

The definition (4.7) of the bracket in the AL scheme is rather unilluminating, and we therefore adopt the diagrammatic description of Fig. 2. In Fig. 2, each arrow stands for one of the Jacobian terms

$$\mu_{nm} \frac{\partial(A, B)}{\partial(a_{x+n}, b_{x+m})} \tag{4.10}$$

in (4.2), where μ is α , β , or γ , and a and b are either u or v . The arrow points from location \mathbf{n} to location \mathbf{m} and carries a weight equal to the coefficient μ_{nm} . (The letters labeling the arrows have no physical meaning,

but serve to facilitate our discussion.) Thus, for example, the a arrow in Fig. 2 stands for the term

$$\alpha_{(-2,1)(-1,2)} \frac{\partial(A, B)}{\partial(u_{x+(-2,1)}, v_{x+(-1,2)})}, \tag{4.11}$$

while the b arrow stands for

$$\gamma_{(1,2)(1,0)} \frac{\partial(A, B)}{\partial(v_{x+(1,2)}, v_{x+(1,0)})}. \tag{4.12}$$

Since, on the C grid, u points and v points never coincide, the diagonal arrows in Fig. 2 correspond to α terms; horizontal arrows correspond to β terms; and vertical arrows correspond to γ terms. For A grid brackets or E grid brackets, these three different types of arrows must be distinguished. The diagrams, which become more useful as the schemes become more complex, display the symmetries of the coefficients much more transparently than definitions like (4.7). We shall see that, because of symmetry, only four of the arrows in Fig. 2 are actually independent. In a sense, therefore, the AL scheme is completely specified by four arrows and their accompanying weights.

Now we address the symmetry properties of the coefficients. Suppose we want to conserve potential entropy in the AL form

$$Z = \frac{1}{2} \sum_{\mathbf{x}} \zeta_{\mathbf{x}}^2 \tilde{h}_{\mathbf{x}}^{-1}, \tag{4.13}$$

where $\zeta_{\mathbf{x}}$ and $\tilde{h}_{\mathbf{x}}$ are given by (4.5)–(4.6). It follows that

$$\hat{U}_{ij} \equiv \partial Z / \partial u_{i,j} = (2\Delta)^{-1} (q_{i,j+1} - q_{i,j-1}), \tag{4.14a}$$

$$\hat{V}_{ij} \equiv \partial Z / \partial v_{i,j} = (2\Delta)^{-1} (q_{i-1,j} - q_{i+1,j}), \tag{4.14b}$$

$$\hat{\Phi}_{ij} \equiv \frac{\partial Z}{\partial h_{i,j}} = -\frac{1}{8} (q_{i+1,j+1}^2 + q_{i+1,j-1}^2 + q_{i-1,j+1}^2 + q_{i-1,j-1}^2). \tag{4.14c}$$

[We reserve the notation U_{ij} , V_{ij} , Φ_{ij} —without hats—for the corresponding derivatives of the Hamiltonian;

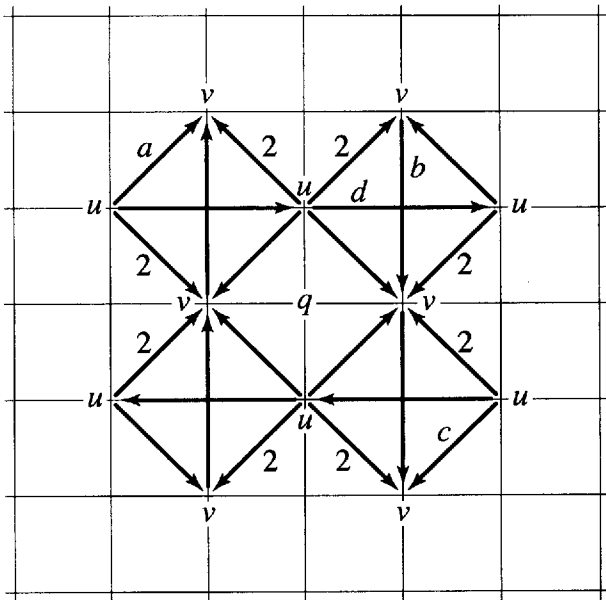


FIG. 2. A diagrammatic description of the AL bracket (4.7). Each of the 24 arrows represents a term in (4.2). The eight arrows labeled with "2" have weight 2/24; all the other arrows have weight 1/24. For a full explanation, see the text.

cf. (2.6) and (5.31).] To conserve (4.13), we must enforce the Casimir property $\{A, Z\} = 0$ for any functional A . Once again, by the chain rule, it suffices to require that $\{u_x, Z\} = \{v_x, Z\} = \{h_x, Z\} = 0$ for every \mathbf{x} . Since our scheme is homogeneous, we may take $\mathbf{x} = \mathbf{0}$ with no loss in generality. Then from (4.1)–(4.3), we find that

$$\begin{aligned} \{h_0, Z\} &= \{h_0, Z\}_R \\ &= (2\Delta)^{-1} [\hat{U}_{(-1,0)} - \hat{U}_{(1,0)} + \hat{V}_{(0,-1)} - \hat{V}_{(0,1)}] \\ &= 0. \end{aligned} \quad (4.15)$$

The last step in (4.15) follows by substitution from (4.14a)–(4.14b). Close examination reveals that (4.15) vanishes because we have used the *same* approximation for first derivatives in (4.3) as in (4.5), and because finite-difference operators commute. Similarly, by (4.1)–(4.3), we find that

$$\begin{aligned} \{u_0, Z\} &= \sum_{\mathbf{n}, \mathbf{m}} q_{-\mathbf{n}} (\alpha_{\mathbf{n}\mathbf{m}} \hat{V}_{-\mathbf{n}+\mathbf{m}} + 2\beta_{\mathbf{n}\mathbf{m}} \hat{U}_{-\mathbf{n}+\mathbf{m}}) \\ &\quad - (2\Delta)^{-1} [\hat{\Phi}_{(1,0)} - \hat{\Phi}_{(-1,0)}], \end{aligned} \quad (4.16)$$

where, with no loss in generality, we have assumed that $\beta_{\mathbf{nm}} = -\beta_{\mathbf{mn}}$. Then, using (4.14), we find that $\{u_0, Z\} = 0$ implies

$$\begin{aligned} (2\Delta)^{-1} \sum_{\mathbf{n}, \mathbf{m}} q_{-\mathbf{n}} [\alpha_{\mathbf{n}\mathbf{m}} (q_{-\mathbf{n}+\mathbf{m}-\mathbf{i}} - q_{-\mathbf{n}+\mathbf{m}+\mathbf{i}}) \\ + 2\beta_{\mathbf{n}\mathbf{m}} (q_{-\mathbf{n}+\mathbf{m}+\mathbf{j}} - q_{-\mathbf{n}+\mathbf{m}-\mathbf{j}})] \\ = -(2\Delta)^{-1} \frac{1}{8} [q_{(2,1)}^2 + q_{(2,-1)}^2 - q_{(-2,1)}^2 - q_{(-2,-1)}^2]. \end{aligned} \quad (4.17)$$

By similar steps, we find that $\{v_0, Z\} = 0$ implies

$$\begin{aligned} (2\Delta)^{-1} \sum_{\mathbf{n}, \mathbf{m}} -q_{-\mathbf{m}} [\alpha_{\mathbf{n}\mathbf{m}} (q_{\mathbf{n}-\mathbf{m}+\mathbf{j}} - q_{\mathbf{n}-\mathbf{m}-\mathbf{j}}) \\ + 2\gamma_{\mathbf{nm}} (q_{\mathbf{n}-\mathbf{m}-\mathbf{i}} - q_{\mathbf{n}-\mathbf{m}+\mathbf{i}})] \\ = -(2\Delta)^{-1} \frac{1}{8} [q_{(1,2)}^2 + q_{(-1,2)}^2 - q_{(1,-2)}^2 - q_{(-1,-2)}^2], \end{aligned} \quad (4.18)$$

where, again, with no loss in generality, we have assumed that $\gamma_{\mathbf{nm}} = -\gamma_{\mathbf{mn}}$. The right-hand side of (4.17) is, as it must be, a finite-difference approximation to $\partial_x (\delta Z / \delta h) = \partial_x (-(1/2)q^2)$. Similarly, the right-hand side of (4.18) is an approximation to $\partial_y (-(1/2)q^2)$.

To obtain a potential-entrophy-conserving scheme we must choose the coefficients $\alpha_{\mathbf{nm}}$, $\beta_{\mathbf{nm}}$, $\gamma_{\mathbf{nm}}$ in such a way that (4.17) and (4.18) are satisfied for arbitrary q_{ij} values. Suppose that the arbitrary q field is altered such that $q_{ij} \rightarrow q_{ji}$. Making this alteration to the q terms in (4.18), and then interchanging the dummy variables $n_x \leftrightarrow m_y$ and $m_x \leftrightarrow n_y$, where $\mathbf{n} = (n_x, n_y)$ and $\mathbf{m} = (m_x, m_y)$, we find that the result is identical to (4.17) if the coefficients obey

$$\alpha(n_x, n_y)(m_x, m_y) = \alpha(m_y, m_x)(n_y, n_x) \quad \text{and} \quad (4.19a)$$

$$\gamma(n_x, n_y)(m_x, m_y) = \beta(m_y, m_x)(n_y, n_x), \quad (4.19b)$$

where we write $\alpha_{(i,j)(k,l)}$ as $\alpha(i, j)(k, l)$ for greater clarity. Thus, solutions α, γ of (4.18) that satisfy (4.19a) automatically satisfy (4.17) with β determined by (4.19b). Next we note that the alteration $q_{ij} \rightarrow q_{-i,j}$ leaves the right-hand side of (4.18) unchanged. The same alteration leaves the left-hand side unchanged if

$$\alpha(n_x, n_y)(m_x, m_y) = \alpha(-n_x, n_y)(-m_x, m_y) \quad \text{and} \quad (4.20a)$$

$$\gamma(n_x, n_y)(m_x, m_y) = -\gamma(-n_x, n_y)(-m_x, m_y). \quad (4.20b)$$

Similarly, $q_{ij} \rightarrow q_{i,-j}$ leads to the symmetry properties

$$\alpha(n_x, n_y)(m_x, m_y) = \alpha(n_x, -n_y)(m_x, -m_y) \quad \text{and} \quad (4.21a)$$

$$\gamma(n_x, n_y)(m_x, m_y) = -\gamma(n_x, -n_y)(m_x, -m_y). \quad (4.21b)$$

To these we add the arbitrary property

$$\gamma(n_x, n_y)(m_x, m_y) = -\gamma(m_x, m_y)(n_x, n_y), \quad (4.22)$$

already imposed.³

We define a *class* to be a set of coefficients whose values are determined by giving the value of one member of the set, and then using the symmetry properties (4.19)–(4.22). For example, each of the four equations in (4.7) refers to the members of a single class. These four classes correspond to four classes of arrows in Fig. 2. The four classes comprise the set of four diagonal arrows closest to the origin, the set of four diagonal arrows furthest from the origin, the remaining diagonal arrows, and all the vertical and horizontal arrows. The symmetry property (4.19a) corresponds to the fact that, if the a arrow in Fig. 2 is reflected across the diagonal through the first and third quadrant, and if its direction is then reversed, it becomes the c arrow. The symmetry property (4.19b) corresponds to the fact that the same operation converts the b arrow into the d arrow. The other symmetry properties have similar interpretations.

We have reduced the problem of finding energy- and potential-entrophy-conserving shallow-water dynamics to two steps. First, we use the symmetry properties (4.19a) and (4.20)–(4.22) to reduce the set of unknown α and γ coefficients to a set containing only one member from each class. Then we solve for the members of this reduced set by requiring that the coefficient of each monomial $q_{\mathbf{n}} q_{\mathbf{m}}$ vanish in (4.18). This yields a large linear system for the reduced set of α and γ coefficients. The size of this system is determined by the stencil size—the range of the sums over \mathbf{n} and \mathbf{m} in (4.2). Once all the α and γ coefficients are determined, we determine the β coefficients from (4.19b). The bracket (4.1)–(4.6) is then completely determined. This determines the discrete dynamics, except for the choice of Hamiltonian. The potential entrophy (4.13) and the energy (i.e., the Hamiltonian) are conserved for any choice of Hamiltonian; (4.8) and (4.9) are two of many possible choices.

³ Unlike (4.19)–(4.21), (4.22) has no physical content; it merely removes a physically undetectable arbitrariness in the γ coefficients.

Except for stencil size, the only arbitrary ingredient of the discrete dynamics is the finite-difference form of q . As already noted, the finite-difference approximation to the numerator of q —the relative vorticity—determines the finite-difference approximation in $\{A, B\}_R$. Only by matching these two approximations, in the sense that (4.3) matches (4.5), do we satisfy the Casimir property $\{h_0, Z\} = 0$. In this paper, we restrict our attention to (4.5), the simplest second-order approximation.

However, the denominator \tilde{h} of q is still completely arbitrary. If instead of (4.6) we use the approximation

$$\begin{aligned} \tilde{h}_{i,j} = & ah_{i,j} + \frac{1}{4}b(h_{i+1,j} + h_{i,j-1} + h_{i-1,j} + h_{i,j+1}) \\ & + \frac{1}{4}c(h_{i+1,j+1} + h_{i-1,j-1} + h_{i-1,j+1} + h_{i+1,j-1}), \end{aligned} \quad (4.23)$$

where a, b, c are any three constants satisfying

$$a + b + c = 1, \quad (4.24)$$

then (4.18) generalizes to

$$\begin{aligned} & \sum_{n,m} q_{-m} [\alpha_{nm}(q_{n-m+j} - q_{n-m-j}) \\ & \quad + 2\gamma_{nm}(q_{n-m-i} - q_{n-m+i})] \\ & = \frac{1}{2}a[q_{(0,1)}^2 - q_{(0,-1)}^2] \\ & \quad + \frac{1}{8}b[q_{(0,2)}^2 + q_{(1,1)}^2 + q_{(-1,1)}^2 - q_{(0,-2)}^2 - q_{(1,-1)}^2 \\ & \quad \quad - q_{(-1,-1)}^2] \\ & \quad + \frac{1}{8}c[q_{(1,2)}^2 + q_{(-1,2)}^2 - q_{(1,-2)}^2 - q_{(-1,-2)}^2]. \end{aligned} \quad (4.25)$$

We require that (4.24)–(4.25) hold for arbitrary q . This yields a large linear system of equations in $k + 3$ unknowns, where k is the number of classes of α and γ coefficients allowed by the truncation in \mathbf{n} and \mathbf{m} , and the three additional unknowns correspond to a, b, c . We call this system of equations the *determining system* of the numerical scheme. Classes contain 1, 2, 4, or 8 members, but the majority of classes contain 8. Thus symmetry considerations reduce the size of the determining system by a factor of almost 16 [considering that symmetry makes (4.17) equivalent to (4.18)]. We find that, for sufficiently large stencil size, the solution of the determining system contains a large number of arbitrary parameters; thus there are a great many energy- and potential-*enstrophy*-conserving shallow-water schemes. The number of schemes increases with the stencil size and would presumably further increase with generalization of (4.5) and (4.23). But before proceeding any further with the two-dimensional case, we recur to the case of one spatial dimension, in which the determining system is easy to solve by hand.

5. Analysis of the one-dimensional case

The one-dimensional analog of (4.1)–(4.5) is

$$\begin{aligned} \{A, B\} = & \sum_i \sum_{n=-\infty}^{\infty} \sum_{m=-\infty}^{\infty} q_i \alpha_{nm} \frac{\partial(A, B)}{\partial(u_{i+n}, v_{i+m})} \\ & + (2\Delta)^{-1} \sum_i \left[\frac{\partial B}{\partial u_i} \left(\frac{\partial A}{\partial h_{i+1}} - \frac{\partial A}{\partial h_{i-1}} \right) \right. \\ & \quad \left. - \frac{\partial A}{\partial u_i} \left(\frac{\partial B}{\partial h_{i+1}} - \frac{\partial B}{\partial h_{i-1}} \right) \right], \end{aligned} \quad (5.1)$$

where

$$q_i = (2\Delta)^{-1}(v_{i-1} - v_{i+1})\tilde{h}_i^{-1} \quad (5.2)$$

is the potential vorticity at the i th grid point, and

$$\begin{aligned} \tilde{h}_i = & ah_i + \frac{1}{2}b(h_{i-1} + h_{i+1}) \\ & + \frac{1}{2}c(h_{i-2} + h_{i+2}) + \dots \end{aligned} \quad (5.3a)$$

with

$$a + b + c + \dots = 1 \quad (5.3b)$$

is a general approximation to h_i , analogous to (4.23). In (5.1) the sum over i represents a sum over all the grid points in the periodic, one-dimensional domain. The sums over n and m have infinite ranges, but we assume that α_{nm} vanishes if the magnitude of n or m exceeds the small prescribed integer M , where M is the stencil size of the numerical scheme.

The dynamics corresponding to (5.1)–(5.3) conserves the potential enstrophy

$$Z = \sum_i (2\Delta)^{-2}(v_{i+1} - v_{i-1})^2 \tilde{h}_i^{-1} \quad (5.4)$$

if $\{u_0, Z\} = \{v_0, Z\} = \{h_0, Z\} = 0$. As in section 3, the last two of these are trivially satisfied in one dimension, and $\{u_0, Z\} = 0$ implies

$$Q = D, \quad (5.5)$$

where

$$Q \equiv \sum_{n=-\infty}^{\infty} \sum_{m=-\infty}^{\infty} q_{-n} \alpha_{nm} (q_{m-n+1} - q_{m-n-1}) \quad \text{and} \quad (5.6)$$

$$\begin{aligned} D \equiv & \frac{1}{2}a(q_1^2 - q_{-1}^2) + \frac{1}{4}b(q_2^2 - q_{-2}^2) \\ & + \frac{1}{4}c(q_3^2 + q_{-1}^2 - q_{-3}^2 - q_1^2) + \dots \end{aligned} \quad (5.7)$$

We also obtain (5.5)–(5.7) (with $b = 1$) directly from (4.17) by deleting the y component of all the vector subscripts in (4.17); note that the β terms then cancel. Similarly, there is no a priori motivation like that in section 4 for inserting β or γ terms in (5.1), because

there are no rotations in one dimension. Thus, the only coefficient symmetry property is the analog,

$$\alpha(n, m) = \alpha(-n, -m), \tag{5.8}$$

of (4.20a), where we write $\alpha(n, m) \equiv \alpha_{nm}$ for clarity.⁴

We must choose the α_{nm} to satisfy (5.5)–(5.7), subject to (5.8), for arbitrary q_i . Clearly, (5.7) can be rewritten in the form

$$D \equiv a_1(q_1^2 - q_{-1}^2) + a_2(q_2^2 - q_{-2}^2) + a_3(q_3^2 - q_{-3}^2) + \dots, \tag{5.9}$$

where a_1, a_2, a_3, \dots are determined by a, b, c, \dots in the obvious way. The normalization condition (5.3b) is equivalent to the requirement that the right-hand side of (5.7) or (5.9) is a consistent approximation to $\Delta\partial_x(q^2)$. By straightforward steps we rewrite (5.6) in the form

$$Q = \sum_{n=-\infty}^{\infty} [\alpha(-n, -1) - \alpha(-n, 1)]q_n^2 + \sum_{n=-\infty}^{\infty} \sum_{r=1}^{\infty} [\alpha(-n, r-1) - \alpha(-n, r+1) + \alpha(-n-r, -r-1) - \alpha(-n-r, -r+1)]q_n q_{n+r}. \tag{5.10}$$

Then (5.5)–(5.10) imply

$$\alpha(n, 1) - \alpha(n, -1) = a_n \tag{5.11}$$

for all n (with $a_{-n} \equiv -a_n$), and

$$\alpha(n, r+1) - \alpha(n, r-1) - \alpha(n-r, -r-1) + \alpha(n-r, -r+1) = 0 \tag{5.12}$$

for all n and all $r \geq 1$. The a_n , which correspond to the choice of the denominator (5.3) in potential vorticity, act as the “forcing term” in the equations (5.11)–(5.12) for the α ’s. To solve (5.11)–(5.12), we define

$$\mu(n, r) \equiv \alpha(n, r-1) - \alpha(n, r+1). \tag{5.13}$$

Then (5.11)–(5.12) take the respective forms

$$\mu(n, 0) = -a_n \quad \text{and} \tag{5.14}$$

$$\mu(n, r) = \mu(r-n, r). \tag{5.15}$$

The general solution of (5.15) is

$$\mu(n, r) = f_r \left(\left| n - \frac{1}{2}r \right| \right), \tag{5.16}$$

where f_r is an arbitrary function defined at integer arguments if r is even, and half-integer arguments if r is odd. Thus, for each n , we have from (5.14) and (5.16) the sequence of equations

⁴ The notation $\alpha(n)(m) \equiv \alpha_{nm}$ would be more consistent with section 4, but is too cumbersome.

$$\alpha(n, -1) - \alpha(n, 1) = a_n,$$

$$\alpha(n, 0) - \alpha(n, 2) = f_1 \left(\left| n - \frac{1}{2} \right| \right),$$

$$\alpha(n, 1) - \alpha(n, 3) = f_2 (|n - 1|),$$

$$\alpha(n, 2) - \alpha(n, 4) = f_3 \left(\left| n - \frac{3}{2} \right| \right),$$

⋮

$$\alpha(n, M-2) - \alpha(n, M) = f_{M-1} \left(\left| n - \frac{M-1}{2} \right| \right),$$

$$\alpha(n, M-1) - 0 = f_M \left(\left| n - \frac{M}{2} \right| \right),$$

$$\alpha(n, M) - 0 = f_{M+1} \left(\left| n - \frac{M+1}{2} \right| \right). \tag{5.17}$$

We see that the equations for $\alpha(n, m)$ with even m decouple from those with odd m . Only the latter feel the forcing term a_n . With no loss in generality we assume that the stencil size M is odd. Then the general solution of (5.17) is easily seen to be

$$\alpha(n, 0) = f_1 + f_3 + \dots + f_M,$$

$$\alpha(n, 2) = f_3 + \dots + f_M,$$

⋮

$$\alpha(n, M-1) = f_M, \tag{5.18}$$

and

$$\alpha(n, -1) = a_n + f_2 + f_4 + \dots + f_{M+1},$$

$$\alpha(n, 1) = f_2 + f_4 + \dots + f_{M+1},$$

$$\alpha(n, 3) = f_4 + \dots + f_{M+1},$$

⋮

$$\alpha(n, M) = f_{M+1}. \tag{5.19}$$

In (5.18) and (5.19) the argument of each f_r is the same as in (5.17). Equations (5.18) and (5.19) give $\alpha(n, m)$ for all n and all positive m . The symmetry property (5.8) then determines $\alpha(n, m)$ for negative m . This same symmetry property imposes two conditions on the otherwise arbitrary f_r . That is, from $\alpha(n, 0) = \alpha(-n, 0)$, we obtain

$$f_1 \left(\left| n + \frac{1}{2} \right| \right) - f_1 \left(\left| n - \frac{1}{2} \right| \right) + f_3 \left(\left| n + \frac{3}{2} \right| \right) - f_3 \left(\left| n - \frac{3}{2} \right| \right) + \dots + f_M \left(\left| n + \frac{M}{2} \right| \right) - f_M \left(\left| n - \frac{M}{2} \right| \right) = 0, \tag{5.20}$$

and from $\alpha(n, 1) = \alpha(-n, -1)$, we obtain

$$\begin{aligned}
& f_2(ln + 1) - f_2(ln - 1) + f_4(ln + 2) \\
& - f_4(ln - 2) + \cdots + f_{M+1} \left(\left| n + \frac{M+1}{2} \right| \right) \\
& - f_M \left(\left| n - \frac{M+1}{2} \right| \right) = a_n. \quad (5.21)
\end{aligned}$$

In overall summary, the general, one-dimensional, potential-entropy-conserving, shallow-water bracket is given by (5.1)–(5.3) and (5.18)–(5.19), where a_n is determined by the form of (5.3), and the functions f_r are arbitrary except for the two constraints (5.20) and (5.21).

To satisfy (5.18) and (5.20), we may choose $f_r = 0$ for all odd r . Then $\alpha(n, m)$ vanishes for all even m . The odd- m solution (5.19) contains arbitrary parameters of the form $f_r(s)$, where r is a positive even integer ($r = 2, 4, 6, \dots$), and s is a nonnegative integer ($s = 0, 1, 2, 3, \dots$). Suppose that only one particular $f_r(s)$ is nonzero. We calculate the corresponding solution. The general solution (5.19) is a superposition of such solutions. The normalization condition (5.21) or (5.11) can be satisfied by an a posteriori scaling of the arbitrary parameters. If only $f_r(s) \neq 0$ then (5.19) implies that the only nonvanishing $\alpha(n, m)$ with positive m are

$$\begin{aligned}
\alpha\left(\frac{r}{2} + s, 1\right) &= \alpha\left(\frac{r}{2} - s, 1\right) = \alpha\left(\frac{r}{2} + s, 3\right) \\
&= \alpha\left(\frac{r}{2} - s, 3\right) = \cdots \\
&= \alpha\left(\frac{r}{2} + s, r - 1\right) \\
&= \alpha\left(\frac{r}{2} - s, r - 1\right). \quad (5.22)
\end{aligned}$$

The simplest such schemes correspond to the smallest values of r and s . For the case $r = 2, s = 0$, the only nonzero coefficients are

$$\alpha(1, 1) = \alpha(-1, -1). \quad (5.23)$$

The size of (5.23) is determined by the normalization condition (5.11) to be

$$\alpha(1, 1) = a_1 = \frac{1}{2}, \quad (5.24)$$

corresponding to $a = 1, b = c = \cdots = 0$ in (5.3). This is the previously found scheme (3.6) and (3.9).

For the case $r = 2, s = 1$, we obtain from (5.22) the nonvanishing coefficients

$$\alpha(2, 1) = \alpha(-2, -1) = \alpha(0, 1) = \alpha(0, -1). \quad (5.25)$$

The normalization requirements (5.11) imply $\alpha(0, 1) = \alpha(0, -1)$, and

$$\alpha(2, 1) = a_2 = \frac{1}{4}b = \frac{1}{4}. \quad (5.26)$$

Thus, $\tilde{h}_i = (1/2)(h_{i-1} + h_{i+1})$ by (5.3). This scheme is the one-dimensional projection of the AL scheme (4.5)–(4.7).

Now consider the scheme corresponding to arbitrary values of r and s . By (5.22) and (5.8) this scheme contains r equal, nonvanishing α 's if $s = 0$, and $2r$ equal, nonvanishing α 's if $s > 0$. The common value of (5.22) is determined by (5.11) in the form

$$\alpha\left(\frac{1}{2}r + s, 1\right) - \alpha\left(\frac{1}{2}r + s, -1\right) = a_{r/2+s}, \quad (5.27a)$$

$$\alpha\left(\frac{1}{2}r - s, 1\right) - \alpha\left(\frac{1}{2}r - s, -1\right) = a_{r/2-s}. \quad (5.27b)$$

The second terms in (5.27a,b) vanish [except in the case $r = 2s$, in which (5.27b) reduces to the identity $\alpha(0, 1) - \alpha(0, -1) = a_0 = 0$]. Thus, when $s = 0$, (5.27) implies that the common value of (5.22) is $a_{r/2}$, which is then the only nonvanishing coefficient in (5.9). When $s > 0$, (5.27) implies that the common value of (5.22) is $a_{r/2+s} = a_{r/2-s}$, which are then the only two nonvanishing coefficients in (5.9). Suppose, for example, that $r = s = 2$. From (5.22) and (5.8), we have the four nonvanishing coefficients

$$\alpha(3, 1) = \alpha(-3, -1) = \alpha(-1, 1) = \alpha(1, -1). \quad (5.28)$$

The normalization requirements (5.27) imply that $a_3 = -a_1 = 1/4$ in (5.9), corresponding to $a = b = 0, c = 1$ in (5.7) and (5.3). The common value of (5.28) is $1/4$, and (5.3) takes the form $\tilde{h}_i = (1/2)(h_{i-2} + h_{i+2})$.

It is perhaps easier to reverse the process of normalization by noting that the nonvanishing α 's must sum to unity. That is, the common value of (5.22) is r^{-1} if $s = 0$, and $(2r)^{-1}$ if $s > 0$. With the α 's thus completely determined, Q is a completely determined sum of squares; that is, the double sum in (5.10) vanishes. It only remains to adjust the coefficients in (5.7) such that $Q = D$; this determines the form of (5.3). The numerical scheme is then completely determined except for the choice of Hamiltonian. This viewpoint shows that the problem of finding one-dimensional, potential-entropy-conserving schemes essentially reduces to the problem of finding α 's consistent with (5.8) that reduce (5.10) to a nontrivial sum of squares.

What happens if nontrivial solutions of (5.18) and (5.20) are included? Since the α 's that solve the forced system (5.19) and (4.21) automatically sum to unity, the α 's that solve the unforced system (5.18) and (5.20) automatically sum to zero. For example, the simplest solution to (5.18) and (5.20) contains the seven nonvanishing coefficients

$$\begin{aligned}
\alpha(0, 0) &= 2\gamma, \\
\alpha(1, 0) &= \alpha(-1, 0) = \gamma, \quad \text{and} \\
\alpha(1, 2) &= \alpha(-1, -2) = \alpha(2, 2) \\
&= \alpha(-2, -2) = -\gamma, \quad (5.29)
\end{aligned}$$

where γ is an arbitrary constant. The numerical scheme corresponding to (5.25), (5.26), and (5.29) is

$$\begin{aligned}
\frac{du_i}{dt} &= \frac{1}{4}(q_{i-2}V_{i-1} + q_{i+2}V_{i+1} + q_iV_{i+1} + q_iV_{i-1}) \\
&+ \gamma(2q_iV_i + q_{i-1}V_{i-1} + q_{i+1}V_{i+1} - q_{i-1}V_{i+1} \\
&\quad - q_{i+1}V_{i-1} - q_{i-2}V_i - q_{i+2}V_i) \\
&- (2\Delta)^{-1}(\Phi_{i+1} - \Phi_{i-1}), \quad (5.30a)
\end{aligned}$$

$$\begin{aligned}
\frac{dv_i}{dt} &= -\frac{1}{4}(q_{i-1}U_{i+1} + q_{i+1}U_{i-1} + q_{i-1}U_{i-1} + q_{i+1}U_{i+1}) \\
&- \gamma(2q_iU_i + q_iU_{i+1} + q_iU_{i-1} - q_{i-2}U_{i-1} \\
&\quad - q_{i+2}U_{i+1} - q_{i-2}U_i - q_{i+2}U_i), \quad (5.30b)
\end{aligned}$$

$$\frac{dh_i}{dt} = -(2\Delta)^{-1}(U_{i+1} - U_{i-1}), \quad (5.30c)$$

where

$$U_i \equiv \partial H / \partial u_i, \quad V_i \equiv \partial H / \partial v_i, \quad \Phi_i \equiv \partial H / \partial h_i, \quad (5.31)$$

and H is the arbitrary discrete Hamiltonian. When $\gamma = 0$, the scheme (5.30) reduces to the one-dimensional version of the AL scheme (for their choice of Hamiltonian). The γ terms, which contribute equal numbers of Coriolis terms of both signs, certainly complicate (5.30), but in the next section we shall see that the ability to adjust γ can sometimes be very useful.

6. Analysis of the two-dimensional case

Now we return to the two-dimensional case. The fundamental equation (4.25) can be written in the form

$$Q = D, \quad (6.1)$$

where

$$\begin{aligned}
Q &= \sum_{\mathbf{m}} \mu(\mathbf{0}, -\mathbf{m}) q_{\mathbf{m}}^2 \\
&+ \sum_{\mathbf{r}} \sum_{\mathbf{m}} [\mu(\mathbf{r}, -\mathbf{m}) - \mu(\mathbf{r}, \mathbf{r} + \mathbf{m})] q_{\mathbf{m}} q_{\mathbf{m}+\mathbf{r}}, \quad (6.2)
\end{aligned}$$

$$\begin{aligned}
\mu(\mathbf{r}, \mathbf{m}) &\equiv \alpha(\mathbf{r} - \mathbf{j}, \mathbf{m}) - \alpha(\mathbf{r} + \mathbf{j}, \mathbf{m}) \\
&+ 2\gamma(\mathbf{r} + \mathbf{i}, \mathbf{m}) - 2\gamma(\mathbf{r} - \mathbf{i}, \mathbf{m}), \quad \text{and} \quad (6.3)
\end{aligned}$$

$$D = \sum_{\mathbf{m}} a_{\mathbf{m}} q_{\mathbf{m}}^2. \quad (6.4)$$

In (6.2), the summation over $\mathbf{m} = (m_x, m_y)$ is over all integers m_x, m_y , while the sum over \mathbf{r} is over the half-plane excluding $\mathbf{r} = \mathbf{0}$. Thus (6.2) is analogous to (5.10), and (6.3) is analogous to (5.13). The coefficients $a_{\mathbf{m}}$ in

(6.4) are determined by the coefficients a, b, c in (4.25) in the same way that (5.7) determines (5.9), hence $a_{\mathbf{m}} = -a_{-\mathbf{m}}$. Since (6.1) must hold for arbitrary $q_{\mathbf{n}}$, it follows that

$$\mu(\mathbf{0}, -\mathbf{m}) = a_{\mathbf{m}} \quad (6.5)$$

for all \mathbf{m} , and

$$\mu(\mathbf{r}, \mathbf{m}) = \mu(\mathbf{r}, \mathbf{r} - \mathbf{m}) \quad (6.6)$$

for all \mathbf{m} and all $\mathbf{r} \neq \mathbf{0}$. The general solution of (6.6) is

$$\mu(\mathbf{r}, \mathbf{m}) = f_{\mathbf{r}}\left(\mathbf{m} - \frac{1}{2}\mathbf{r}\right), \quad (6.7)$$

where $f_{\mathbf{r}}(\mathbf{s})$ is an arbitrary function with the properties $f_{\mathbf{r}}(\mathbf{s}) = f_{\mathbf{r}}(-\mathbf{s})$ and $f_{\mathbf{r}}(\mathbf{s}) = -f_{-\mathbf{r}}(\mathbf{s})$. Equation (6.7) is analogous to (5.16). Combining (6.5) and (6.7) with the definition (6.3), we obtain the analog

$$\begin{aligned}
\alpha(\mathbf{r} - \mathbf{j}, \mathbf{m}) - \alpha(\mathbf{r} + \mathbf{j}, \mathbf{m}) + 2\gamma(\mathbf{r} + \mathbf{i}, \mathbf{m}) \\
- 2\gamma(\mathbf{r} - \mathbf{i}, \mathbf{m}) &= \begin{cases} a_{\mathbf{m}}, & \mathbf{r} = \mathbf{0} \\ f_{\mathbf{r}}\left(\mathbf{m} - \frac{1}{2}\mathbf{r}\right), & \mathbf{r} \neq \mathbf{0} \end{cases} \quad (6.8)
\end{aligned}$$

of (5.17). By the symmetry properties (4.19), (6.8) implies

$$\begin{aligned}
\alpha(\mathbf{m}, \mathbf{r} - \mathbf{i}) - \alpha(\mathbf{m}, \mathbf{r} + \mathbf{i}) + 2\beta(\mathbf{m}, \mathbf{r} + \mathbf{j}) \\
- 2\beta(\mathbf{m}, \mathbf{r} - \mathbf{j}) &= \begin{cases} a_{\mathbf{m}^*}, & \mathbf{r} = \mathbf{0} \\ f_{\mathbf{r}^*}\left(\mathbf{m}^* - \frac{1}{2}\mathbf{r}^*\right), & \mathbf{r} \neq \mathbf{0}, \end{cases} \quad (6.9)
\end{aligned}$$

where $(m_x, m_y)^* \equiv (m_y, m_x)$. The set (6.9) bears the same relation to (4.17) as does (6.8) to (4.18). Either set, (6.8) or (6.9), combined with the symmetry conditions (4.19)–(4.22), completely determines the discrete bracket.

I have not succeeded in solving (6.8) or (6.9) by hand, as (5.17) was solved to yield (5.18)–(5.21). Instead we resort to machine manipulations. However, we can deduce some important properties of the solutions directly from (6.8) and (6.9). Like (5.17), the set (6.8) decouples into independent subsets of equations. The subset corresponding to $\mathbf{r} = (\text{even}, \text{even})$ is analogous to (5.19), and it alone feels the forcing terms $a_{\mathbf{m}}$. The other three subsets are analogous to (5.18). By (6.8) and (6.9), this forced subset involves only $\alpha(\mathbf{n}, \mathbf{m})$ with $\mathbf{n} = (\text{even}, \text{odd})$ and $\mathbf{m} = (\text{odd}, \text{even})$, $\gamma(\mathbf{n}, \mathbf{m})$ with $\mathbf{n}, \mathbf{m} = (\text{odd}, \text{even})$, and $\beta(\mathbf{n}, \mathbf{m})$ with $\mathbf{n}, \mathbf{m} = (\text{even}, \text{odd})$. In other words, the directly forced scheme corresponds to a C system. Thus the α, β, γ coefficients corresponding to E- or A-grid arrangements of the variables can be set to zero a priori, with no effect on our ability to satisfy (6.8) or (6.9), just as

(5.17) is most easily satisfied by setting the coefficients in (5.18) to zero. This step would reduce the size of (6.8) or (6.9) by about a factor 4. Furthermore, since $\mathbf{m} = (\text{odd}, \text{even})$ in (6.8) and (6.9), we can expect to find solutions only for the case $a = b = 0, c = 1$ in (4.23)–(4.25). This property that the simplest schemes satisfying (6.8) or (6.9) are C schemes is a direct consequence of the choice (4.5) for the numerator of q_{ij} . As emphasized in section 4, this choice, which determines the form of the left-hand sides of (6.8) and (6.9), is the only arbitrary component (besides the stencil size) of schemes based on (4.2).

We solve for schemes by demanding that (4.25) hold for arbitrary values of the q 's, subject to the symmetry requirements (4.19)–(4.22), in the manner outlined at the end of section 4. A relatively simple computer program assembles the quadratic form in (4.25); uses the symmetry requirements to eliminate all of the α and γ coefficients except for a single coefficient in each class; forms the determining system of equations by demanding that the coefficient of each monomial $q_n q_m$ vanish; solves for the α and γ coefficients and the constants a, b, c ; assembles the Poisson bracket; and checks the resulting schemes for accuracy and potential-estrophy conservation.

In presenting results, it is convenient to specify the value of a single member of each class of coefficients, the values of the other members being determined by (4.19)–(4.21) but not (4.22). That is, in presenting our results, we drop the arbitrary property (4.22) used to simplify the equations in section 4.⁵ With this understood, the AL bracket is defined by

$$\alpha(2, 1)(1, 0) = \frac{1}{12},$$

$$\alpha(0, 1)(1, 0) = \alpha(2, 1)(1, 2) = \gamma(1, 2)(1, 0) = \frac{1}{24}. \tag{6.10}$$

The specification (6.10) is equivalent to (4.7) and to Fig. 2.

We present results for the stencil shown in Fig. 3. That is, we assume that the sums over \mathbf{n} and \mathbf{m} in (4.2) are over the 25 values of (n_x, n_y) depicted in Fig. 3. The determining system corresponding to Fig. 3 comprises 461 equations in 193 unknowns. Other, larger, stencils were also investigated, but the general scheme corresponding to Fig. 3 is already quite large—containing 22 free parameters!—and is certainly large enough to illustrate general properties of the schemes. As expected from our discussion of (6.8) and (6.9), we find that $a = b = 0$ and $c = 1$; the denominator of q_{ij} takes

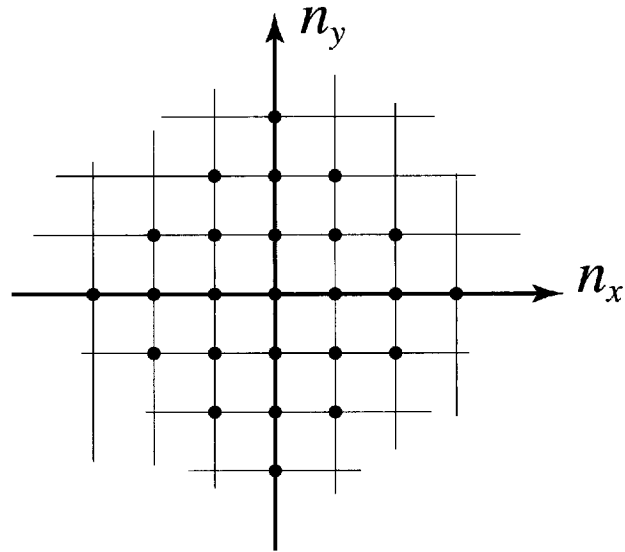


FIG. 3. The stencil for the numerical schemes discussed in section 6. Each of the sums over \mathbf{n} and \mathbf{m} in (4.2) runs over the 25 values of (n_x, n_y) represented in the figure.

the form (4.6). The “forced” coefficients conform to the C grid. For the chosen stencil, these coefficients take the forms

$$\gamma(1, 2)(-1, 2) = \gamma_1 \tag{4}, \tag{6.11a}$$

$$\gamma(1, 2)(-1, 0) = \gamma_2 \tag{8}, \tag{6.11b}$$

$$\gamma(1, 2)(1, 0) = \frac{1}{24} + \gamma_2 \tag{8}, \tag{6.11c}$$

$$\gamma(1, 2)(1, -2) = -\gamma_2 \tag{4}; \tag{6.11d}$$

and

$$\alpha(2, 1)(1, 2) = \frac{1}{24} \tag{4}, \tag{6.12a}$$

$$\alpha(0, 1)(1, 0) = \frac{1}{24} + 2\gamma_1 \tag{4}, \tag{6.12b}$$

$$\alpha(2, 1)(1, 0) = \frac{1}{12} + \gamma_2 \tag{8}, \tag{6.12c}$$

$$\alpha(2, 1)(3, 0) = -\gamma_1 - \gamma_2 \tag{8}, \tag{6.12d}$$

$$\alpha(2, 1)(-1, 0) = \gamma_2 \tag{8}, \tag{6.12e}$$

$$\alpha(2, 1)(1, -2) = -\gamma_2 \tag{8}, \tag{6.12f}$$

where γ_1 and γ_2 are arbitrary constants. Once again, each of (6.11)–(6.12) specifies the values of an entire class of α or γ coefficients. The square bracket after each equation gives the size of the class, which is equal to the number of Coriolis terms contributed by the class to each momentum equation. The solution (6.11)–(6.12) is analogous to (5.19) after normalization (5.21). The constants γ_1 and γ_2 are analogous

⁵ Thus, (6.10) implies $\gamma(1, 0)(1, 2) = 0$, and not $\gamma(1, 0)(1, 2) = -1/24$.

to the f , on the right-hand side of (5.19). (Only two such constants survive truncation to the chosen stencil size.) The AL scheme corresponds to $\gamma_1 = \gamma_2 = 0$. The scheme proposed by TW corresponds to $\gamma_1 = 1/24$ and $\gamma_2 = 0$.

In addition to the C-grid coefficients (6.11)–(6.12), the general scheme corresponding to the stencil in Fig. 3 contains a 20-parameter set of “unforced” coefficients, analogous to (5.18); 8 of these 20 are E-grid solutions inconsistent with the C-grid; 12 of the 20 are A-grid schemes inconsistent with the E-grid and the C-grid. Appendix A lists the simplest of the 20 non-C-grid solutions. These include one especially simple solution:

$$\gamma(1, 1)(-1, 1) = \gamma_3 \quad [4], \quad (6.13a)$$

$$\alpha(0, 1)(0, 0) = \gamma_3 \quad [4], \quad (6.13b)$$

$$\alpha(2, 0)(3, 0) = -\gamma_3 \quad [4], \quad (6.13c)$$

containing only three classes and 12 Coriolis terms; and the somewhat more complicated solution:

$$\gamma(1, 1)(0, 1) = \gamma_4 \quad [8], \quad (6.14a)$$

$$\alpha(2, 0)(2, 0) = -\gamma_4 \quad [4], \quad (6.14b)$$

$$\alpha(1, 0)(2, 0) = -\gamma_4 \quad [4], \quad (6.14c)$$

$$\alpha(1, 0)(0, 0) = \gamma_4 \quad [4], \quad (6.14d)$$

$$\alpha(0, 0)(0, 0) = 4\gamma_4 \quad [1], \quad (6.14e)$$

which is interesting because it is one of the few schemes involving the *nonstaggered* term (6.14e). None of the 20 unforced solutions contains constant terms like those in (6.11) and (6.12).

As in the one-dimensional case, we satisfy (6.8)–(6.9) most easily by discarding all the unforced solutions, that is, by setting γ_3, γ_4 , and the remaining 18 free parameters to zero. The surviving scheme is then completely summarized by (6.11) and (6.12). We study (6.11)–(6.12) as a representative subset—a “microcosm”—of the larger set of all conserving schemes. Then we consider the more general scheme (6.11)–(6.14).

Equations (6.11)–(6.12) represent a two parameter set of shallow-water schemes that conserve mass, circulation, energy and potential enstrophy. Each point in the γ_1 – γ_2 plane shown in Fig. 4 corresponds to one such scheme. All the points not on solid lines (including the axes) correspond to schemes involving all 10 of the classes in (6.11)–(6.12); such schemes have 64 Coriolis terms of the form $q_{ij}V_{mn}$ or $q_{ij}U_{mn}$ in each momentum equation. Points on the solid lines in Fig. 4 correspond to schemes in which at least one of the 10 classes in (6.11)–(6.12) is absent. In fact, four classes vanish along the γ_1 axis in Fig. 4, while one class vanishes along each of the other solid lines. The simpler schemes, comprising fewer classes, lie at the intersections of the solid lines in Fig. 4. The

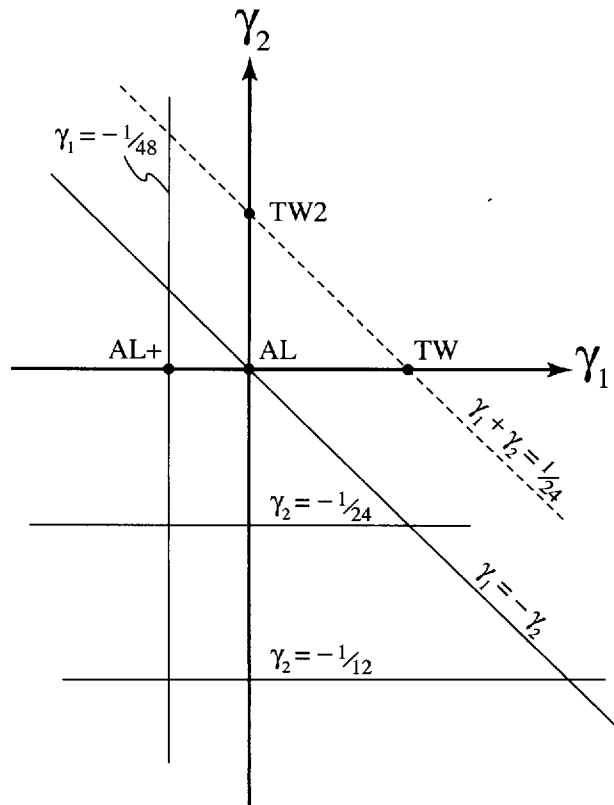


FIG. 4. Every point on the γ_1 – γ_2 plane corresponds to an energy- and potential-enstrophy-conserving scheme defined by (6.11)–(6.12). All are consistent with the C grid. The Arakawa–Lamb (AL) scheme, at the origin, is the simplest such scheme; AL+ is the second simplest. The Takano–Wurtele (TW) scheme and the TW2 scheme lie on the (dashed) line of schemes with fourth-order accuracy in the vorticity equation.

AL scheme, at the origin, lies at the intersection of the γ_1 axis (with four vanishing classes), the γ_2 axis (with one vanishing class), and the line $\gamma_1 = -\gamma_2$ (with one vanishing class). It is the simplest scheme, with only four classes and 24 Coriolis terms. The next simplest scheme, at $\gamma_1 = -1/48, \gamma_2 = 0$, contains 5 classes and 32 Coriolis terms. All the other schemes with $\gamma_2 = 0$, including TW, contain 6 classes and 36 Coriolis terms. All the schemes with $\gamma_2 \neq 0$ contain at least 8 classes.

Since no choice of γ_1 and γ_2 can make all of (6.11) vanish, all of the schemes on Fig. 4 contain unphysical Coriolis terms of the kind originally introduced by AL. Since the additional, non-C-grid solutions like (6.13) and (6.14) do not affect (6.11), this fact remains generally true: *All potential-enstrophy-conserving schemes contain unphysical Coriolis terms.* Likewise we shall show that all potential-enstrophy-conserving schemes have only second-order accuracy in the grid-spacing Δ .

Appendix B gives the explicit finite-difference formulas corresponding to the scheme (6.11)–(6.14). By Taylor expanding these formulas in the usual way, we obtain

$$\begin{aligned} \frac{\partial u}{\partial t} = & -\Phi_x + qV - \frac{1}{6}\Delta^2\Phi_{xxx} \\ & + \frac{1}{6}\Delta^2(3qV_{xx} + 3qV_{yy} + 6q_{xx}V + 6q_xV_x + 3q_{yy}V - 4q_yU_x - 2q_{xy}U) \\ & + 4(2\gamma_1 + 2\gamma_2 + \gamma_3 + \gamma_4)\Delta^2(q_xV_x - q_{xx}V - 2q_{yy}V - q_yV_y - q_{xy}U - 2q_xU_y) + O(\Delta^4), \end{aligned} \quad (6.15a)$$

$$\begin{aligned} \frac{\partial v}{\partial t} = & -\Phi_y - qU - \frac{1}{6}\Delta^2\Phi_{yyy} \\ & - \frac{1}{6}\Delta^2(3qU_{xx} + 3qU_{yy} + 6q_{yy}U + 6q_yU_y + 3q_{xx}U - 4q_xV_y - 2q_{xy}V) \end{aligned} \quad (6.15b)$$

$$- 4(2\gamma_1 + 2\gamma_2 + \gamma_3 + \gamma_4)\Delta^2(q_yU_y - q_{yy}U - 2q_{xx}U - q_xU_x - q_{xy}V - 2q_yV_x) + O(\Delta^4), \quad \text{and}$$

$$\frac{\partial h}{\partial t} = -U_x - V_y - \frac{1}{6}\Delta^2(U_{xxx} + V_{yyy}) + O(\Delta^4). \quad (6.15c)$$

To fully assess (6.15), we must express q , $U \equiv \delta H/\delta u$, $V \equiv \delta H/\delta v$, and $\Phi \equiv \delta H/\delta h$ in terms of u , v , and h . The potential vorticity q , defined by (4.4)–(4.6), is then a further source of $O(\Delta^2)$ truncation error. On the other hand, the further error introduced by U , V , and Φ depends upon the choice of Hamiltonian. The choice (4.9) introduces no further truncation error, while (4.8) introduces a further $O(\Delta^2)$ truncation error. Quite apart from these issues, it is obvious from (6.15) that no choice of the γ 's can completely cancel the $O(\Delta^2)$ terms. In particular, the accuracy of (6.15c) cannot be improved. More surprisingly, we note that the leading-order truncation error associated with each of the four free parameters γ_1 , γ_2 , γ_3 , γ_4 has exactly the same form. This means that, insofar as accuracy is concerned, we can (for example) do nothing by adjusting γ_2 that we cannot do by adjusting γ_1 . Then, since the most complicated schemes with $\gamma_2 = 0$ are simpler than the simplest schemes with $\gamma_2 \neq 0$, there would seem, from the standpoint of accuracy and conservation properties alone, to be no reason whatsoever to consider schemes with $\gamma_2 \neq 0$.

Remarkably, this *rule of proportional truncation error* seems to be generally true. We find that 19 of the 22 free parameters in the general scheme corresponding to the stencil in Fig. 3 contribute an $O(\Delta^2)$ truncation error proportional to that in (6.15a–b), while 3 of the 22 parameters contribute no $O(\Delta^2)$ error at all. If this were not the case, that is, if the different parameters contributed different forms of truncation error, then it might be possible to adjust the parameters to cancel much of the error in the momentum equations. Instead it seems that one adjustable parameter is as good as many, and that we may as well consider only those single parameters that correspond to the simplest schemes.

Using an approach similar to AL, TW obtained a potential-ensrophy-conserving scheme with $O(\Delta^4)$ accu-

racy in the vorticity equation *only*, provided that the mass flux could be assumed nondivergent, $U_x + V_y = 0$. The TW scheme, which corresponds to the point $\gamma_1 = 1/24$, $\gamma_2 = 0$ in Fig. 4, is subject to two important caveats. First, the vorticity itself retains only second-order accuracy in Δ . Second, the condition $U_x + V_y = 0$ is imposed with only second-order accuracy. To recover the TW result, we first note that (4.5) implies that

$$\zeta = (v_x - u_y) + \frac{1}{6}\Delta^2(v_{xxx} - u_{yyy}) + O(\Delta^4), \quad (6.16)$$

and thus

$$\begin{aligned} \zeta_i = & \left(\partial_x + \frac{1}{6}\Delta^2\partial_{xx} + \dots \right) v_i \\ & - \left(\partial_y + \frac{1}{6}\Delta^2\partial_{yy} + \dots \right) u_i + O(\Delta^4). \end{aligned} \quad (6.17)$$

Then, putting

$$\begin{aligned} U = & -(2\Delta)^{-1}(\psi_{i,j+1} - \psi_{i,j-1}) \\ = & -\psi_y - \frac{1}{6}\Delta^2\psi_{yyy} + O(\Delta^4), \end{aligned} \quad (6.18a)$$

$$\begin{aligned} V = & (2\Delta)^{-1}(\psi_{i+1,j} - \psi_{i-1,j}) \\ = & \psi_x + \frac{1}{6}\Delta^2\psi_{xxx} + O(\Delta^4) \end{aligned} \quad (6.18b)$$

in (6.15) and substituting the result into (6.17), we find that

$$\zeta_i = -\psi_x q_y + \psi_y q_x + O(\Delta^4), \quad (6.19)$$

provided that

$$2\gamma_1 + 2\gamma_2 + \gamma_3 + \gamma_4 = \frac{1}{12}, \quad (6.20)$$

where each coefficient occurs, as it must, in the same

TABLE 1. Summary of numerical solutions depicted in Fig. 6.

Scheme	γ_1	γ_2	γ_3	γ_4	Classes	Coriolis terms	Accuracy	Symmetry
AL	0	0	0	0	4	24	Second order	C grid
AL+	$-\frac{1}{48}$	0	0	0	5	32	Second order	C grid
TW	$\frac{1}{24}$	0	0	0	6	36	Fourth order	C grid
TW2	0	$\frac{1}{24}$	0	0	9	60	Fourth order	C grid
TW3	0	0	$\frac{1}{12}$	0	7	36	Fourth order	A grid
TW4	0	0	0	$\frac{1}{12}$	9	45	Fourth order	A grid

proportion as in (6.15a) and (6.15b). If (6.20) is satisfied, then schemes of the general form (6.11)–(6.14) have fourth-order accuracy in the vorticity equation. The equation corresponding to (6.20) for the most general scheme based on our chosen lattice contains 19 free parameters. Thus pseudo-fourth-order schemes occupy a 19-dimensional space!

If we once again restrict ourselves to schemes of the form (6.11)–(6.12), then the fourth-order schemes lie on the dashed line $\gamma_1 + \gamma_2 = 1/24$ on Fig. 4. The TW scheme lies at the intersection of this line with $\gamma_2 = 0$. With its 6 classes and 36 Coriolis terms, TW is by far the simplest fourth-order scheme on Fig. 4; all other schemes on the dashed line contain at least 9 classes of coefficients. However, the A-grid fourth-order scheme with $\gamma_3 = 1/12$ and $\gamma_1 = \gamma_2 = \gamma_4 = 0$ contains only 7 classes and 36 Coriolis terms—the same number as TW.

To assess the performance of the schemes, we compare results from numerical experiments using the six schemes given in Table 1. These include: the simplest (AL) and second-simplest (AL+) second-order C-grid-brackets, the simplest fourth-order C-bracket (TW), and a much more complicated fourth-order C-bracket (TW2). All four of these schemes are shown on Fig. 4. We also test the fourth-order A-bracket TW3, which is the only fourth-order bracket as simple as TW, and the more complicated fourth-order A-bracket TW4. Each of these six schemes comprises the AL “core” plus terms proportional to one of the four γ 's. In every case except AL+, the γ terms are chosen to give the scheme fourth-order accuracy in the vorticity equation. In the case of AL+, γ_1 is chosen to cancel (6.12b) by introducing (6.11a) and (6.12d); once again, this is the second-simplest scheme after AL. The terms proportional to each γ are shown diagrammatically in Fig. 5, using the same arrow conventions as in Fig. 2. Figure 5 shows more clearly than any mathematical formula that the four schemes TW1, TW2, TW3, and TW4 achieve fourth-order accuracy by adding very different types of Coriolis terms to the AL core.

Figure 6 shows the potential vorticity field in numerical solutions using the six schemes defined in Table 1. The common initial conditions are parallel shear layers slightly perturbed by a sinusoidal cross flow. All six solutions use the simple Hamiltonian (4.9) and thus are

technically A-grid schemes. All have the same small Navier–Stokes viscosity. At the time shown in Fig. 6, the viscosity has reduced the energy by less than 0.02% and the potential enstrophy by about 13%. Some further details of the calculations are given in appendix B. Figure 6 shows that, despite significant differences among the schemes, the solutions are very similar, with the biggest differences between the two second-order schemes at the top of Fig. 6 and the four fourth-order schemes at the bottom.

The “rule of proportional truncation error” noted above must surely have its source in the exactly conserving nature of our schemes. Exact conservation means conservation to all orders in Δ . Thus, the fact that (6.11)–(6.14) conserves energy for arbitrary values of $\gamma_1, \gamma_2, \gamma_3, \gamma_4$ means that

$$\iint d\mathbf{x}(\Phi h_t + Uu_t + Vv_t) = 0 \quad (6.21)$$

for arbitrary Φ, U , and V , if h_t, u_t , and v_t are replaced by the terms proportional to $\Delta^2 \gamma_i$ in (6.15). Similarly, conservation of potential enstrophy implies that

$$\iint d\mathbf{x} \left[\left(\partial_x + \frac{1}{6} \Delta^2 \partial_{xx} + \dots \right) v_t - \left(\partial_y + \frac{1}{6} \Delta^2 \partial_{yy} + \dots \right) u_t \right] = O(\Delta^4), \quad (6.22)$$

following the same substitution [cf. (6.17)]. The steps required to verify (6.21) and (6.22), which involve many integrations by parts, evidently require that the truncation error associated with each γ_i take the very particular, common form in (6.15). Since this same commonality represents an obstacle to the construction of higher-order schemes, the requirements of conservation and accuracy are seen to be somewhat antagonistic.

The search for *genuinely* fourth-order conserving schemes must begin by replacing the finite differences in (4.3) and (4.5) by fourth-order differences. Such a search yielded a fourth-order, conserving bracket for the one-dimensional shallow-water equations, but

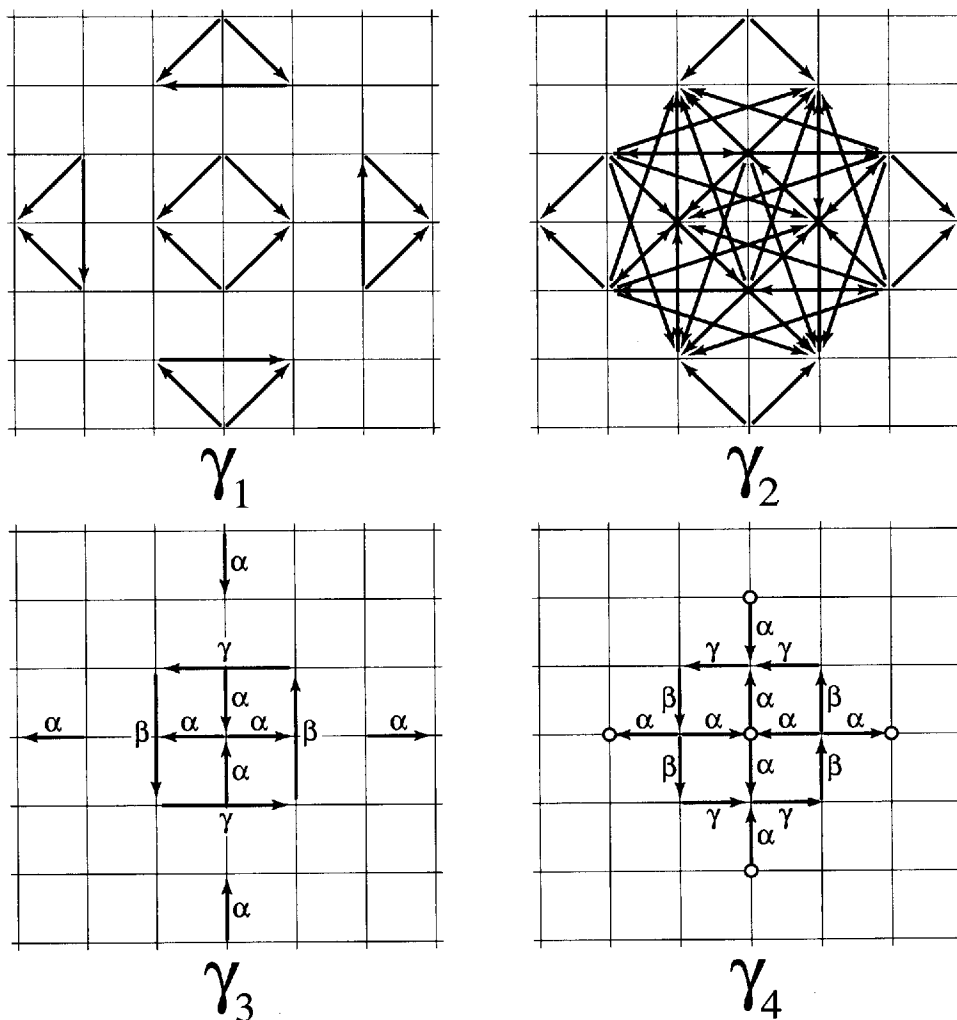


FIG. 5. Diagrammatic representation of the terms in (4.2) proportional to each of the free parameters $\gamma_1, \gamma_2, \gamma_3, \gamma_4$ in numerical schemes of the general form (6.11)–(6.14). The general scheme comprises the AL core (Fig. 2) plus an arbitrary weighting of each of the four diagrams on this figure. Since the γ_1 and γ_2 terms are consistent with the C grid, the meaning of the arrows in the top two diagrams is—as in Fig. 2—unambiguous. In the two bottom diagrams, each arrow is labeled as an $\alpha, \beta,$ or γ term. The small circles on the γ_4 diagram represent the α terms corresponding to (6.14b) and (6.14e). These may be regarded as arrows that begin and end at the same point. For clarity, the relative weight of each arrow is not shown. This figure is primarily intended to depict the very different structures of the arbitrary components of (6.11)–(6.14).

only at the relatively large stencil size of $M = 7$. Two-dimensional searches failed for stencil sizes up to $M = 9$.

I also searched for schemes that conserve other mo-

ments of the potential vorticity, besides potential enstrophy. If we ask that the dynamics (4.1)–(4.5) and (4.23)–(4.24) conserve the analog of $\lambda^{-1} \iint dx hq^\lambda$, then the coefficients in (4.2) and (4.23) must satisfy

$$\begin{aligned} \sum_{n,m} q_{-m} [\alpha_{nm}(q_{n-m+j}^{\lambda-1} - q_{n-m-j}^{\lambda-1}) + 2\gamma_{nm}(q_{n-m-1}^{\lambda-1} - q_{n-m+1}^{\lambda-1})] \\ = \lambda^{-1}(\lambda - 1) \{ a[q_{(0,1)}^\lambda - q_{(0,-1)}^\lambda] + \frac{1}{4} b[q_{(0,2)}^\lambda + q_{(1,1)}^\lambda + q_{(-1,1)}^\lambda - q_{(0,-2)}^\lambda - q_{(1,-1)}^\lambda - q_{(-1,-1)}^\lambda] \\ + \frac{1}{4} c[q_{(1,2)}^\lambda + q_{(-1,2)}^\lambda - q_{(1,-2)}^\lambda - q_{(-1,-2)}^\lambda] \} \end{aligned} \tag{6.23}$$

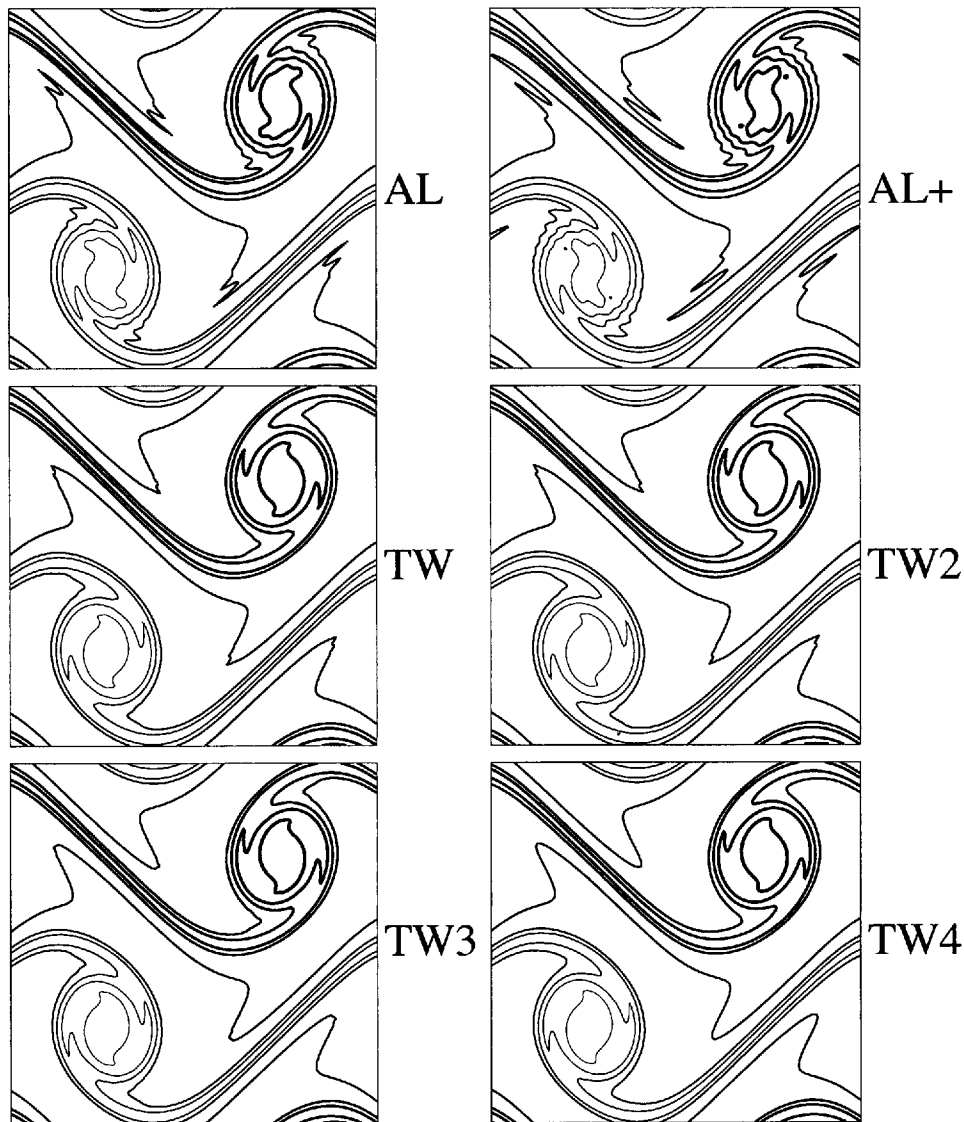


FIG. 6. The potential vorticity field corresponding to an initial condition of slightly perturbed shear layers, as computed by the six distinct energy- and potential- enstrophy-conserving schemes summarized in Table 1. The two schemes at the top have second-order accuracy in the grid spacing. The other four schemes have fourth-order accuracy in the vorticity equation.

for arbitrary values of the q 's. When $\lambda = 2$ (6.23) reduces to (4.25). No solutions of (6.23) were found for $\lambda = 3$ or 4. This is perhaps unsurprising, because for given \mathbf{n} , \mathbf{m} (6.23) contains monomials of the form $q_n q_m^{\lambda-1}$, as well as $q_n^{\lambda-1} q_m$. Thus, when $\lambda = 3$ or 4, the determining system is roughly twice as large as when $\lambda = 2$.

7. Philosophy

For better or worse, the day of the pure theoretician in our field is long past. Research in geophysical fluid dynamics now primarily involves the numerical simulation of fluid motions. Yet despite huge advances in

computer hardware, the methodology of software construction has hardly changed in 50 years. This construction normally proceeds in two stages. In the first stage, we introduce approximate *differential* equations that express the underlying physics. In the second stage, we replace the differential equations with *discrete* analogs using well-established techniques that often rely on ideas about smoothness and the use of Taylor series. These techniques are usually of a kind that could be applied to almost any set of nonlinear partial differential equations.

However, the equations of fluid motion are of a very particular type. In their inviscid form, they possess Hamiltonian structure, with a very distinctive set of

symmetry properties and conservation laws. The conservation laws express the fundamental physics more perfectly than does the typical discrete approximation to the differential equations, designed, as it usually is, to apply equally well to nonconserving equations. It therefore seems preferable to construct the discrete dynamics directly on the basis of the conservation laws alone, without actually writing—and with no pretense at solving—a set of partial differential equations. Of course, *in hindsight* it will always be true that the resulting discrete dynamics is a logical finite-difference approximation to a consistent set of differential equations, just as the dynamics (6.11)–(6.14) correctly limits on (6.15). However, it may be equally true that, in the *construction* of discrete dynamics, the introduction of differential equations can never be more than a misleading distraction.

This somewhat iconoclastic viewpoint finds support in the popularity and success of lattice-gas models and the closely related lattice-Boltzmann method. However, lattice-Boltzmann models do not seem adaptable to conservation laws besides mass and momentum, and, somewhat contrary to popular belief, cannot be constructed on the basis of local conservation laws alone; on the latter point, see especially Dellar (2002). In fact, disillusionment with the lattice-Boltzmann method largely motivated the present work. The present method, like the lattice-Boltzmann method, scarcely invokes the concept of spatial derivative; in fact (4.3) and (4.5) contain the only finite differences involved. However, the present, Poisson-bracket approach seems adaptable to almost any dynamics, whereas the lattice-Boltzmann approach seems fundamentally limited to systems resembling the Navier–Stokes equations.

Nonetheless, we must admit that, although our results are, on the one hand, much more general than those of AL and TW, and on the other hand, more streamlined

than those of Abramopoulos (1988), the ansatz (4.1)–(4.3) copies their common basic strategy of postulating a general form with a great many undetermined weights and then determining the weights in such a way that conservation laws survive. Such an approach is clumsy, wasteful of effort, and seems incapable of finding schemes with genuine fourth-order accuracy or schemes conserving additional Casimirs. Moreover, one-dimensional results like (3.13) suggest that the corresponding two-dimensional form may be very hard to *guess*. What is really needed is a purely *constructive* method of determining Poisson brackets, free of undetermined weights, that can—with sufficient effort—attain any level of accuracy and accommodate any number of conservation laws. Strenuous efforts to find such a constructive method have failed, but I have no doubt that it exists. In the meantime, the present paper is offered as one small step in what is perceived to be the right direction.

Acknowledgments. This work was supported by the National Science Foundation Grant OCE-0100868. I gratefully acknowledge very helpful advice from A. Arakawa, P. J. Dellar, D. A. Randall, and W. H. Schubert.

APPENDIX A

Summary of Solutions

The general energy- and potential-enstrophy-conserving shallow-water scheme corresponding to (4.1)–(4.3) and the stencil in Fig. 3 comprises (6.11)–(6.12) with its 2 free parameters, plus expressions involving 20 additional free parameters. Here, we record the simplest of these 20 additional contributions, namely those involving five or fewer classes of α and γ coefficients. They are

$$\gamma(1, 2, 1, 1) = -\gamma(1, 1, 1, -1) \quad [12] \quad (\text{A.1})$$

$$\alpha(0, 1, 0, 0) = -\alpha(2, 0, 3, 0) = \gamma(1, 1, -1, 1) \quad [12] \quad (\text{A.2})$$

$$\frac{1}{4}\alpha(0, 0, 0, 0) = \alpha(1, 0, 0, 0) = -\alpha(1, 0, 2, 0) = -\alpha(2, 0, 2, 0) = \gamma(1, 1, 0, 1) \quad [21] \quad (\text{A.3})$$

$$\alpha(1, 0, -1, 0) = \alpha(1, 0, 1, 0) = -\alpha(1, 0, 3, 0) = -\alpha(3, 0, 3, 0) = \gamma(2, 1, 0, 1) \quad [24] \quad (\text{A.4})$$

$$\alpha(2, 0, 0, 0) = \alpha(1, 0, 0, 0) = -\alpha(3, 0, 2, 0) = -\alpha(0, 2, 0, 0) = \gamma(2, 1, 1, 1) \quad [28] \quad \text{and} \quad (\text{A.5})$$

$$\frac{1}{2}\alpha(0, 1, 0, 0) = \alpha(1, 1, 0, 0) = -\alpha(1, 1, 2, 0) = -\alpha(2, 1, 2, 0) = \gamma(1, 2, 0, 2) \quad [36] \quad (\text{A.6})$$

Equations (A.1)–(A.6) are analogous to (5.25) except that (A.1)–(A.6) contain only one representative member of each class. The square bracket after each of (A.1)–(A.6) contains the number of Coriolis terms contributed

to each momentum equation. None of (A.1)–(A.6) is consistent with the C grid; only (A.4) is consistent with the E grid. Solution (A.1) contributes only unphysical Coriolis terms, and because it contributes no $O(\Delta^2)$ trun-

cation error, it cannot be used to construct higher-order schemes. Solution (A.2) is equivalent to (6.13), and (A.3) is equivalent to (6.14). The remaining 14 solutions (not shown) contain between 6 and 22 classes of coefficients.

APPENDIX B

Dynamical Equations

In explicit form, the numerical scheme corresponding to (6.11)–(6.14) is

$$\frac{d}{dt}h_{0,0} = -(2\Delta)^{-1}(U_{1,0} - U_{-1,0} + V_{0,1} - V_{0,-1}) \quad \text{and} \tag{B.1}$$

$$\begin{aligned} \frac{d}{dt}u_{0,0} = & -(2\Delta)^{-1}(\Phi_{1,0} - \Phi_{-1,0}) \\ & + \frac{1}{24}[(2q_{2,1} + 2q_{0,-1} + q_{0,1} + q_{2,-1})V_{1,1} + (2q_{0,1} + 2q_{2,-1} + q_{0,-1} + q_{2,1})V_{1,-1} \\ & + (2q_{-2,1} + 2q_{0,-1} + q_{-2,-1} + q_{0,1})V_{-1,1} + (2q_{0,1} + 2q_{-2,1} + q_{-2,-1} + q_{0,-1})V_{-1,-1} \\ & + (q_{0,-1} + q_{2,-1} - q_{2,1} - q_{0,1})U_{2,0} + (q_{0,1} + q_{-2,1} - q_{-2,-1} - q_{0,-1})U_{-2,0}] \\ & + \gamma_1[(2q_{0,1} - q_{0,3} - q_{2,1})V_{1,1} + (2q_{0,-1} - q_{-2,-1} - q_{0,-3})V_{1,-1} + (2q_{0,1} - q_{0,3} - q_{2,1})V_{-1,1} \\ & + (2q_{0,-1} - q_{2,-1} - q_{0,-3})V_{-1,-1} + (q_{-2,1} - q_{2,1})U_{0,2} + (q_{2,-1} - q_{-2,-1})U_{0,-2}] \\ & + \gamma_2[(q_{2,1} + q_{0,-1} - q_{0,3} - q_{-2,1})V_{1,1} + (q_{0,1} + q_{2,-1} - q_{-2,-1} - q_{0,-3})V_{1,-1} \\ & + (q_{0,-1} + q_{-2,1} - q_{0,3} - q_{2,1})V_{-1,1} + (q_{-2,-1} + q_{0,1} - q_{2,-1} - q_{0,-3})V_{-1,-1} + (q_{0,1} - q_{2,1})V_{1,3} \\ & + (q_{0,-1} - q_{2,-1})V_{1,-3} + (q_{0,1} - q_{-2,1})V_{-1,3} + (q_{0,-1} - q_{-2,-1})V_{-1,-3} + (q_{2,1} - q_{-2,-1})V_{3,1} \\ & + (q_{2,-1} - q_{-2,1})V_{3,-1} + (q_{2,1} - q_{-2,-1})V_{-3,1} + (q_{-2,-1} - q_{-2,1})V_{-3,-1} \\ & + (q_{0,-1} + q_{2,-1} - q_{0,1} - q_{2,1})U_{2,0} + (q_{0,1} + q_{-2,1} - q_{2,-1} - q_{0,-1})U_{-2,0} + (q_{2,1} - q_{-2,-1})U_{4,0} \\ & + (q_{-2,-1} - q_{-2,1})U_{-4,0} + (q_{0,1} - q_{2,1})U_{2,2} + (q_{2,-1} - q_{0,-1})U_{2,-2} + (q_{-2,1} - q_{0,1})U_{-2,2} \\ & + (q_{0,-1} - q_{-2,-1})U_{-2,-2}] \\ & + \gamma_3[(q_{0,-1} - q_{0,-3})V_{0,-1} + (q_{0,0} - q_{2,0})V_{-1,0} + (q_{0,0} - q_{-2,0})V_{1,0} + (q_{0,1} - q_{0,3})V_{0,1} \\ & + (q_{-1,1} - q_{1,1})U_{0,2} + (q_{1,-1} - q_{-1,-1})U_{0,-2}] \\ & + \gamma_4[(4q_{0,0} - q_{0,-2} - q_{0,2} - q_{-2,0} - q_{2,0})V_{0,0} + (q_{1,0} - q_{-1,0})V_{1,0} + (q_{-1,0} - q_{1,0})V_{-1,0} + (q_{0,0} - q_{0,2})V_{0,1} \\ & + (q_{0,0} - q_{0,-2})V_{0,-1} + (q_{-1,0} + q_{-1,1} - q_{1,0} - q_{1,1})U_{0,1} + (q_{1,0} + q_{1,-1} - q_{-1,-1} - q_{-1,0})U_{0,-1}], \tag{B.2} \end{aligned}$$

where $u_{i,j}$ is the value of u at the ij grid point, and $U_{ij} = \partial H/\partial u_{ij}$, $V_{ij} = \partial H/\partial v_{ij}$, and $\Phi_{ij} = \partial H/\partial h_{ij}$ are approximations to hu , hv , and Φ , respectively, that depend on the choice of Hamiltonian. To save space, the formulas are written for dh_{00}/dt and du_{00}/dt , but the generalization to dh_{ij}/dt and du_{ij}/dt is obvious. The formula for dv_{00}/dt is obtained from (B.2) as follows. In (B.2), interchange the symbols u and v ; interchange U and V ; interchange all subscripts; and reverse the sign of every q . Thus,

$$\begin{aligned} \frac{d}{dt}v_{0,0} = & -(2\Delta)^{-1}(\Phi_{0,1} - \Phi_{0,-1}) \\ & - \frac{1}{24}[(2q_{1,2} + 2q_{-1,0} + q_{1,0} + q_{-1,2})U_{1,1} \\ & + (2q_{1,0} + 2q_{-1,2} + q_{-1,0} + q_{1,2})U_{-1,1} \\ & + \dots] \tag{B.3} \end{aligned}$$

The numerical solutions depicted in Fig. 6 use the Hamiltonian (4.9) and an eddy viscosity of the form $\partial(hu)/\partial t = \dots \nu \nabla \cdot (h \nabla u)$, which conserves momentum and dissipates energy. The resolution is 200×200 , and the time derivative has been computed using second-order Runge–Kutta.

REFERENCES

Abramopoulos, F., 1988: Generalized energy and potential enstrophy conserving finite difference schemes for the shallow water equations. *Mon. Wea. Rev.*, **116**, 650–662.
 Arakawa, A., 1966: Computational design for long-term numerical integration of the equations of fluid motion: Part I. *J. Comput. Phys.*, **1**, 119–143.
 —, and V. R. Lamb, 1977: Computational design of the basic dynamical processes of the UCLA general circulation model. *Methods Comput. Phys.*, **17**, 174–265.

- , and ——, 1981: A potential enstrophy and energy conserving scheme for the shallow water equations. *Mon. Wea. Rev.*, **109**, 18–36.
- Dellar, P. J., 2002: Non-hydrodynamic modes and an a priori construction of shallow-water lattice Boltzmann equations. *Phys. Rev.*, **65E**, 036309, doi:10.1103/PhysRevE.65.036309.
- Morrison, P. J., 1998: Hamiltonian description of the ideal fluid. *Rev. Mod. Phys.*, **70**, 467–521.
- Ringler, T. D., and D. A. Randall, 2002: A potential enstrophy and energy conserving numerical scheme for solution of the shallow-water equations on a geodesic grid. *Mon. Wea. Rev.*, **130**, 1397–1410.
- Salmon, R., 1988: Semi-geostrophic theory as a Dirac-bracket projection. *J. Fluid Mech.*, **196**, 345–358.
- , 1998: *Lectures on Geophysical Fluid Dynamics*. Oxford University Press, 372 pp.
- , and L. D. Talley, 1989: Generalizations of Arakawa's Jacobian. *J. Comput. Phys.*, **83**, 247–259.
- Shepherd, T. G., 1990: Symmetries, conservation laws, and Hamiltonian structure in geophysical fluid dynamics. *Advances in Geophysics*, Vol. 32, Academic Press, 287–338.
- Szunyogh, I., 1993: Finite-dimensional quasi-Hamiltonian structure in simple model equations. *Meteor. Atmos. Phys.*, **52**, 49–57.
- Takano, K., and M. G. Wurtele, 1982: A fourth-order energy and potential enstrophy conserving difference scheme. Air Force Geophysics Laboratory Tech. Rep. AFGL-TR-82-0205, 85 pp.
- Zeitlin, V., 1991: Finite-mode analogs of 2D ideal hydrodynamics: Coadjoint orbits and local canonical structure. *Physica D*, **49**, 353–362.